creative commons
COMMONS DEED

저작자표시-비영리-변경금지 2.0 대한민국

이용자는 아래의 조건을 따르는 경우에 한하여 자유롭게

- 이 저작물을 복제, 배포, 전송, 전시, 공연 및 방송할 수 있습니다.

다음과 같은 조건을 따라야 합니다:

저작자표시. 귀하는 원저작자를 표시하여야 합니다.

비영리. 귀하는 이 저작물을 영리 목적으로 이용할 수 없습니다.

변경금지. 귀하는 이 저작물을 개작, 변형 또는 가공할 수 없습니다.

- 귀하는, 이 저작물의 재이용이나 배포의 경우, 이 저작물에 적용된 이용허락조건을 명확하게 나타내어야 합니다.
- 저작권자로부터 별도의 허가를 받으면 이러한 조건들은 적용되지 않습니다.

저작권법에 따른 이용자의 권리는 위의 내용에 의하여 영향을 받지 않습니다.

이것은 이용허락규약(Legal Code)을 이해하기 쉽게 요약한 것입니다.

Disclaimer

dCollection

A Doctoral Dissertation

Protective Effects of Phenolic Bioactive Molecules against Particulate Matter-Induced Skin Cell Damage

Ao Xuan Zhen

Department of Medicine

Graduate School

Jeju National University

February 2023

제주대학교 중앙도서관
JEJU NATIONAL UNIVERSITY LIBRARY

미세먼지로 인한 피부세포 손상에 대한 페놀성 화합물의 보호효과

지도교수 현 진 원

진 오 현

이 논문을 의학 박사학위 논문으로 제출함

2022 년 12 월

진오현의 의학 박사학위 논문을 인준함

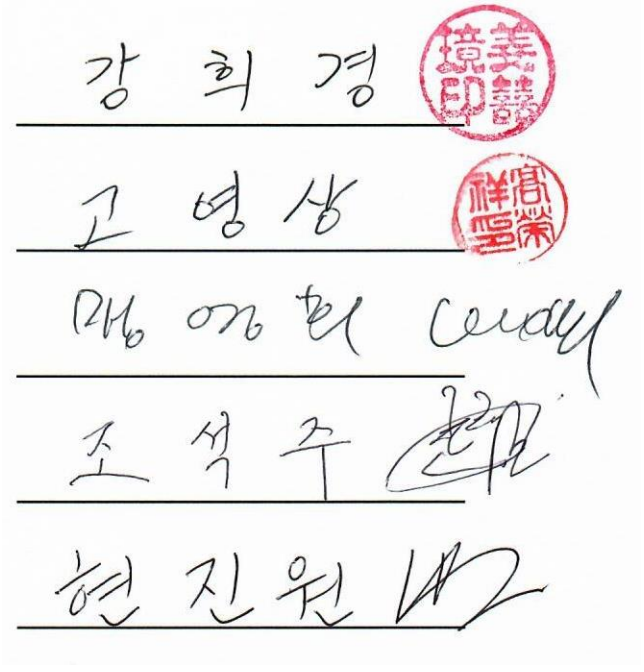

제주대학교 대학원

2022 년 12 월

제주대학교 중앙도서관
JEJU NATIONAL UNIVERSITY LIBRARY

Protective Effects of Phenolic Bioactive Molecules against Particulate Matter-Induced Skin Cell Damage

Ao Xuan Zhen

(Supervised by Professor Jin Won Hyun)

A thesis submitted in partial fulfillment of the requirement for the degree of Doctor of Philosophy in Medicine

2022.12

This thesis has been examined and approved.

Thesis director: Heeteyong Kang

Kohyoung Sung

Younghee Kaeng

Sukgyu Lee

Jin Won Hyun

Approved date Dec 07, 2022

Department of Medicine

GRADUATE SCHOOL

JEJU NATIONAL UNIVERSITY

제주대학교 중앙도서관
JEJU NATIONAL UNIVERSITY LIBRARY

BACKGROUNDS

Air pollution has been an inevitable issue throughout the whole world, especially in developing countries. The ambient particulate matter (PM) differs in size, $PM_{2.5}$, coarse PM, and PM_{10} (aerodynamic diameter less than 2.5 μm, 2.5-10 μm, or less than 10 μm, respectively) (Guarnieri & Balmes, 2014). It has been reported that fine PM ($PM_{2.5}$) could remain floating in the air for several days and invade the human body (Kim *et al.*, 2015). And $PM_{2.5}$ possibly penetrates through the skin, blood-brain, and air-blood barrier (Magnani *et al.*, 2016; Kang *et al.*, 2021; Li *et al.*, 2019). $PM_{2.5}$ was mainly sourced from urban air pollution (traffic, industries, and combustions), which accounts for over 50% of $PM_{2.5}$ contributions over 11 cities distributed in Eastern European and Central Asian countries (Almeida *et al.*, 2020). Transition metals and PAHs, contained in PM, possess special effects to emerge a potential of oxidative stress and contribute to many of the phenotypical alterations of skin barrier functions (Misra *et al.*, 2020; Magnani *et al.*, 2016). In the experiment about skin absorption of metals from road dust, the absorption profile of lead and cobalt were the highest and lowest in intact skin, respectively (Magnano *et al.*, 2022). The electronic microscopy analysis revealed that PAHs are attached to the surfaces of particle cores since the smaller particles have a relatively larger surface area, which tends to be more contribution to increasing the toxic potential (Marrot, 2018). And review has concluded that PAHs contributed notably to carcinogenicity and mutagenicity, and certain PAH derivatives possessed higher toxicity than those of their parent PAHs (Yang *et al.*, 2021).

PM is exposed to animals or humans mainly through ingestion, inhalation, and dermal absorption, which are considered the main pathways to health risks. Previous research concluded that poor air quality has been correlated with pathological effects on many organs, including the integumentary system (Schraufnagel *et al.*, 2019). It is well known that the skin is the largest and most complex organ for human beings, which consists of the epidermis, dermis, hypodermis, and skin appendages (e.g., hairs, sebaceous glands, sweat glands, and

제주대학교 중앙도서관
JEJU NATIONAL UNIVERSITY LIBRARY

nails) (Gu *et al.*, 2020). Airborne pollution has been a deleterious substance resulting in skin aging, aggravation of skin inflammation, and hair loss (Diao *et al.*, 2021; Jun *et al.*, 2020). When skin cells were exposed to PM, numerous adverse responses could be observed, such as keratinocytes apoptosis, fibroblast senescence, melanin genesis, and mast cell activation (Dijkhoff *et al.*, 2020; Grether-Beck *et al.*, 2021; Jin *et al.*, 2019). It has been reported that reactive oxygen species (ROS) are tightly related to health outcomes, such as inflammation, fibrogenesis, tumor growth, metastasis, and cell death (Sun *et al.*, 2020). While intracellular-generated ROS has an important role in regulating cell signals, many pieces of research have demonstrated that $PM_{2.5}$ could induce extra unbearable ROS via disrupting intracellular redox axis balance in skin cells (Hyun *et al.*, 2019; Piao *et al.*, 2018; Zhen *et al.*, 2019a). Moreover, $PM_{2.5}$-induced ROS triggered a major mechanism, which leads to detrimental effects such as skin cancer, skin aging, and inflammation (Peng *et al.*, 2019; Ryu *et al.*, 2019a; Ryu *et al.*, 2019b). What's more, experimental and epidemiological data analysis revealed that inflammation has also been recognized as the main factor for aggregating skin barrier damage (Bae *et al.*, 2020; Ngoc *et al.*, 2017; Kim *et al.*, 2021).

The bioactive compounds, phenolic compounds widely exist in plants, which contained one or more hydroxyl groups on aromatic rings and share a high biological value in various disease treatments (Hu *et al.*, 2021). The natural polyphenols of diphlorethohydroxycarmalol (DPHC) and eckol are abundant in brown seaweed and a plant phenol of purpurogallin (PG) could be obtained from oak nutgall, all of which show various functional effects (Heo *et al.*, 2008; Monteiro *et al.*, 2022; Li *et al.*, 2022). Therefore, this thesis assessed the protective effects of these three phenolic compounds (DPHC, eckol, and PG) on $PM_{2.5}$-induced damage in human keratinocytes.

제주대학교 중앙도서관
JEJU NATIONAL UNIVERSITY LIBRARY

ABBREVIATION

AM: Acetoxymethyl ester; ATGs: Autophagy-related genes; Bax: Bcl-associated X protein; Bcl-2: B-cell lymphoma-2; CHOP: CCAAT-enhancer-binding protein homologous protein; DHR123: Dihydrorhodamin 123; DPPH: 2,2-Diphenyl-1-picrylhydrazyl; DPPP: Diphenyl-1-pyrenylphosphine; ER: Endoplasmic reticulum; ERK: Extracellular signal-regulated kinase; ESR: electron spin resonance; GRP78: Glucose-regulated protein 78; H_2DCFDA: Dichlorodihydrofluorescein diacetate; H_2O_2: Hydrogen peroxide; IRE1: Serine/threonine-protein kinase/endoribonuclease inositol-requiring enzyme 1; JNK: c-Jun N-terminal kinase; LC3: Light chain 3; MAPK: Mitogen-activated protein kinase; MEK: Ras/Raf/Mitogen-activated protein kinase/ERK kinase;MMP: Matrix metalloproteinase; MTT: 3-(4,5-Dimethylthiazol-2-yl)-2,5-diphenyltetrazolium bromide; PAHs: Polycyclic aromatic hydrocarbons; PERK: Protein kinase R-like ER kinase; PI: Propidium iodide; $PM_{2.5}$: Particulate matter 2.5; ROS: Reactive oxygen species; TRITC: Tetramethylrhodamine isothiocyanate; UVB: Ultraviolet B.

제주대학교 중앙도서관
JEJU NATIONAL UNIVERSITY LIBRARY

CONTENTS

제주대학교 중앙도서관
JEJU NATIONAL UNIVERSITY LIBRARY

제주대학교 중앙도서관
JEJU NATIONAL UNIVERSITY LIBRARY

LIST OF FIGURES

제주대학교 중앙도서관
JEJU NATIONAL UNIVERSITY LIBRARY

제주대학교 중앙도서관
JEJU NATIONAL UNIVERSITY LIBRARY

PART I

Diphlorethohydroxycarmalol Inhibited Fine Particulate Matter-Induced Skin Cells Injury via MAPK Signaling Pathway

This work has been published as titled “Diphlorethohydroxycarmalol Attenuates Fine Particulate Matter-Induced Subcellular Skin Dysfunction” in Marine Drugs (2019;17:95).

제주대학교 중앙도서관
JEJU NATIONAL UNIVERSITY LIBRARY

ABSTRACT

Diphlorethohydroxycarmalol (DPHC), a phenolic-based compound is abundant in the brown alga, which shows high potential for antioxidative stress. Here, the protective effect of DPHC on $PM_{2.5}$-induced skin cell damage was evaluated both *in vitro* and *in vivo*. First of all, DPHC scavenged $PM_{2.5}$-induced intracellular ROS, which caused macromolecule damage such as DNA, protein, and lipids in HaCaT keratinocytes and HR-1 hairless mice. In addition, increased epidermal height in $PM_{2.5}$-exposed mice's dorsal skin was prevented by treatment with DPHC. DPHC also reversed $PM_{2.5}$-induced organelles dysfunction, including ER stress, mitochondrial depolarization, and autophagy activation. Moreover, $PM_{2.5}$ induced keratinocytes apoptosis by activation of the MAPK signaling pathway. However, DPHC inhibited the phosphorylation of MAPK signaling-related proteins, ERK, p38, and JNK, thus reducing apoptotic bodies. And the MAPK inhibitors also proved that DPHC protected skin cells from $PM_{2.5}$-induced apoptosis via the MAPK signaling pathway. Therefore, DPHC regulated the activation of MAPK signaling may play a vital role in $PM_{2.5}$-induced skin injury.

KEYWORDS

Diphlorethohydroxycarmalol, $PM_{2.5}$, keratinocytes, skin cell injury, MAPK

제주대학교 중앙도서관
JEJU NATIONAL UNIVERSITY LIBRARY

INTRODUCTION

Fine particles with a diameter of 2.5 to 10 μm or less can easily enter human external organs like the skin, ears, eyes, and nose. And among which the skin exhibited the biggest surface to attach the floating PM (Huang *et al.*, 2018). Additionally, several studies have shown that PM can enter the skin cells and trigger oxidative stress (Puri *et al.*, 2017). As a result, the skin barrier is either directly or indirectly harmed, thickening the skin and bringing on wrinkles (Kim *et al.*, 2016). Also, pathologic events in the skin occur when PM compromises the integrity of the skin, resulting in processes like apoptosis (Morita, 2007). The MAPK signaling pathway, which is likely connected to skin inflammation, can be triggered when skin cells are overexposed to PM (Bosch *et al.*, 2015). Additionally, PM ingredients can promote ROS development, which in turn causes inflammation, whereas the phenolic can reduce ROS production by preventing the activation of MAPKs (Tsai *et al.*, 2017).

The diphlorethohydroxycarmalol (DPHC) is found in the edible seaweed *Ishige okamurae* (a type of brown algae) which is well-recognized for its functional activities (Heo *et al.*, 2008). This compound has been demonstrated to have anticancer, antioxidant, anti-inflammatory, antidiabetic, and antibacterial properties in previous investigations (Kang *et al.*, 2015a; Mayer *et al.*, 2005). In addition, we have previously discussed the mechanism that DPHC can prevent UVB-induced cell damage in human keratinocytes by reducing ROS production and inactivating MAPK signaling pathway (Piao *et al.*, 2013; Piao *et al.*, 2015a). To assess the potential protective effects of DPHC against $PM_{2.5}$-induced skin damage, the oxidation of macromolecules and dysfunction of organelles induced by $PM_{2.5}$ were evaluated both *in vitro* and *in vivo*, and DPHC showed protective effects via the MAPK signaling pathway.

제주대학교 중앙도서관
JEJU NATIONAL UNIVERSITY LIBRARY

RESULTS

Diphlorethohydroxycarmalol (DPHC) prevented $PM_{2.5}$-induced ROS overexpression

According to the cell viability assay, there is no cytotoxicity of DPHC (0, 2.5, 5, 10, 20, and 40 μM) against HaCaT keratinocytes (Figure 1A). DPHC at concentrations of 0, 2.5, 5, 10, 20, or 40 μM, respectively, scavenged free radicals in a dose-dependent manner, and the N-acetylcysteine (NAC, 1 mM) was a positive antioxidant (Figure 1B). According to the scavenging ability of free radicals, 20 μM DPHC was selected as the optimal concentration for the next experiments. The result showed that the $PM_{2.5}$-treated group indicated a high level of intracellular ROS, which was inhibited by treatment with DPHC (Figure 1C). And it was reconfirmed by detecting ROS level with flow cytometry, that DPHC prevented $PM_{2.5}$-induced ROS generation in keratinocytes (Figure 1D). Thus, DPHC highly stopped $PM_{2.5}$-induced ROS production.

제주대학교 중앙도서관
JEJU NATIONAL UNIVERSITY LIBRARY

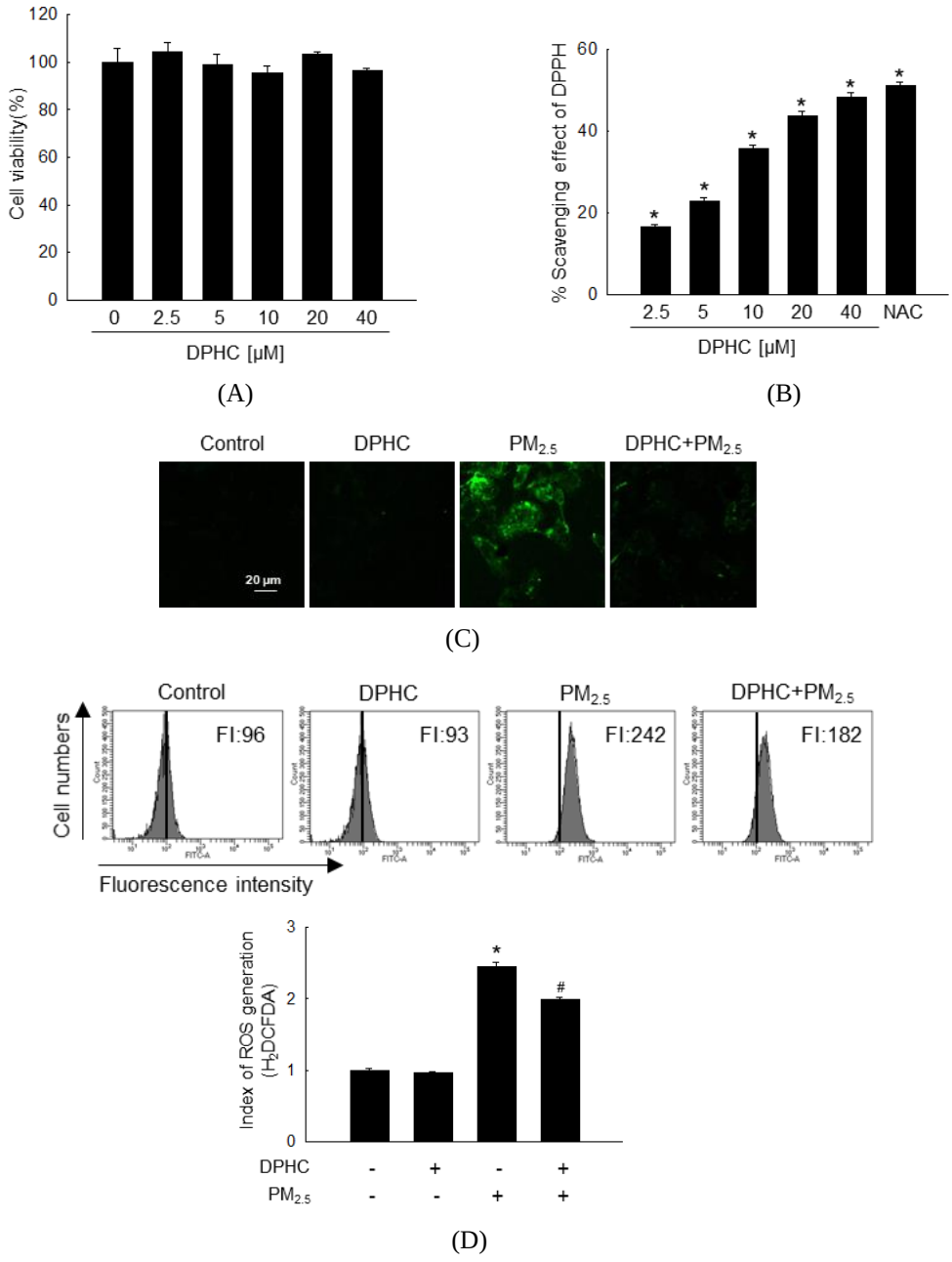

Figure 1. DPHC decreased free radical production. (A) The cell viability was assessed using MTT after cell treatment with DPHC at concentrations of 0, 2.5, 5, 10, 20, and 40 μM for 24 h. (B) The DPPH free radical scavenging of DPHC at concentrations of 0, 2.5, 5, 10, 20, and 40 μM was measured by the DPPH test. *p < 0.05 vs. DPPH. Inhibition of DPHC for intracellular ROS induced by $PM_{2.5}$ was labeled by H_2DCFDA staining by (C)confocal microscopy and (D) flow cytometry. *p < 0.05 and #p < 0.05 vs. control and $PM_{2.5}$-treated group, respectively.

제주대학교 중앙도서관
JEJU NATIONAL UNIVERSITY LIBRARY

DPHC suppressed $PM_{2.5}$-induced cellular macromolecules oxidation both in vitro and in vivo

The fluorescent indicating lipid peroxidation showed a high level in $PM_{2.5}$-exposed cells, whereas the intensity was inhibited by treatment with DPHC (Figure 2A). In addition, DPHC alleviated cellular DNA damage that shielded the formation of $PM_{2.5}$-induced condensed 8-oxoguanine (Figure 2B), prevented $PM_{2.5}$-induced DNA strands breaking (Figure 2C), and inhibited $PM_{2.5}$-induced overexpression of phospho-histone H2A.X (Figure 2D). $PM_{2.5}$ also raised the level of protein carbonylation in keratinocytes, which was reduced by DPHC treatment (Figure 2E). In terms of *in vivo* experiments, DPHC both in a low dose (200 μM) and a high dose (2 mM) decreased the $PM_{2.5}$-induced creation of lipid peroxidation (Figure 2F) and protein carbonyl (Figure 2G). What's more, according to the histological analysis, the dorsal skin in the $PM_{2.5}$ treatment group exhibited a higher epidermis; whereas DPHC in high dose significantly mitigated the height of the epidermis (Figure 2H). Overall, DPHC decreased oxidative stress and prevented skin damage caused by $PM_{2.5}$ both *in vitro* and *in vivo*.

제주대학교 중앙도서관
JEJU NATIONAL UNIVERSITY LIBRARY

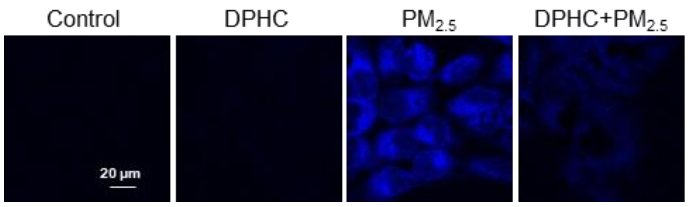

(A)

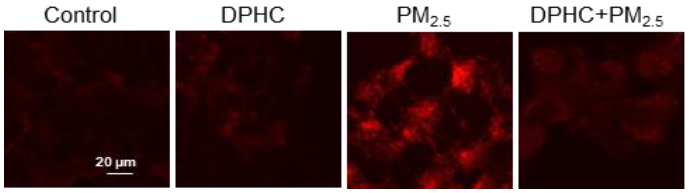

(B)

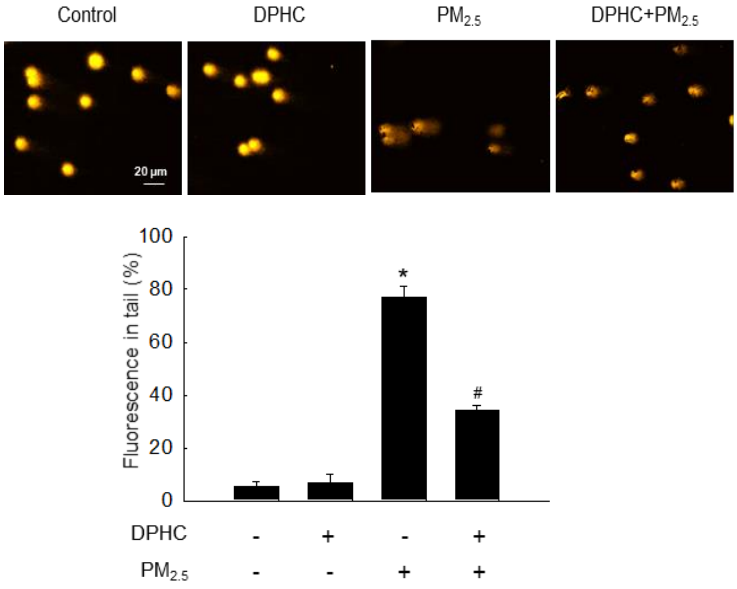

(C)

Figure 2. Cells were guarded by DPHC from macromolecule damage brought on by $PM_{2.5}$. (A) Lipid peroxidation was examined using confocal microscopy following DPPP labeling. (B) Confocal microscopy was used to identify the amount of avidin-TRITC bound to 8-oxoguanine in DNA. (C) DNA damage was assessed using the comet assay. *$p < 0.05$ and #$p < 0.05$ vs. control and $PM_{2.5}$-treated group, respectively.

제주대학교 중앙도서관
JEJU NATIONAL UNIVERSITY LIBRARY

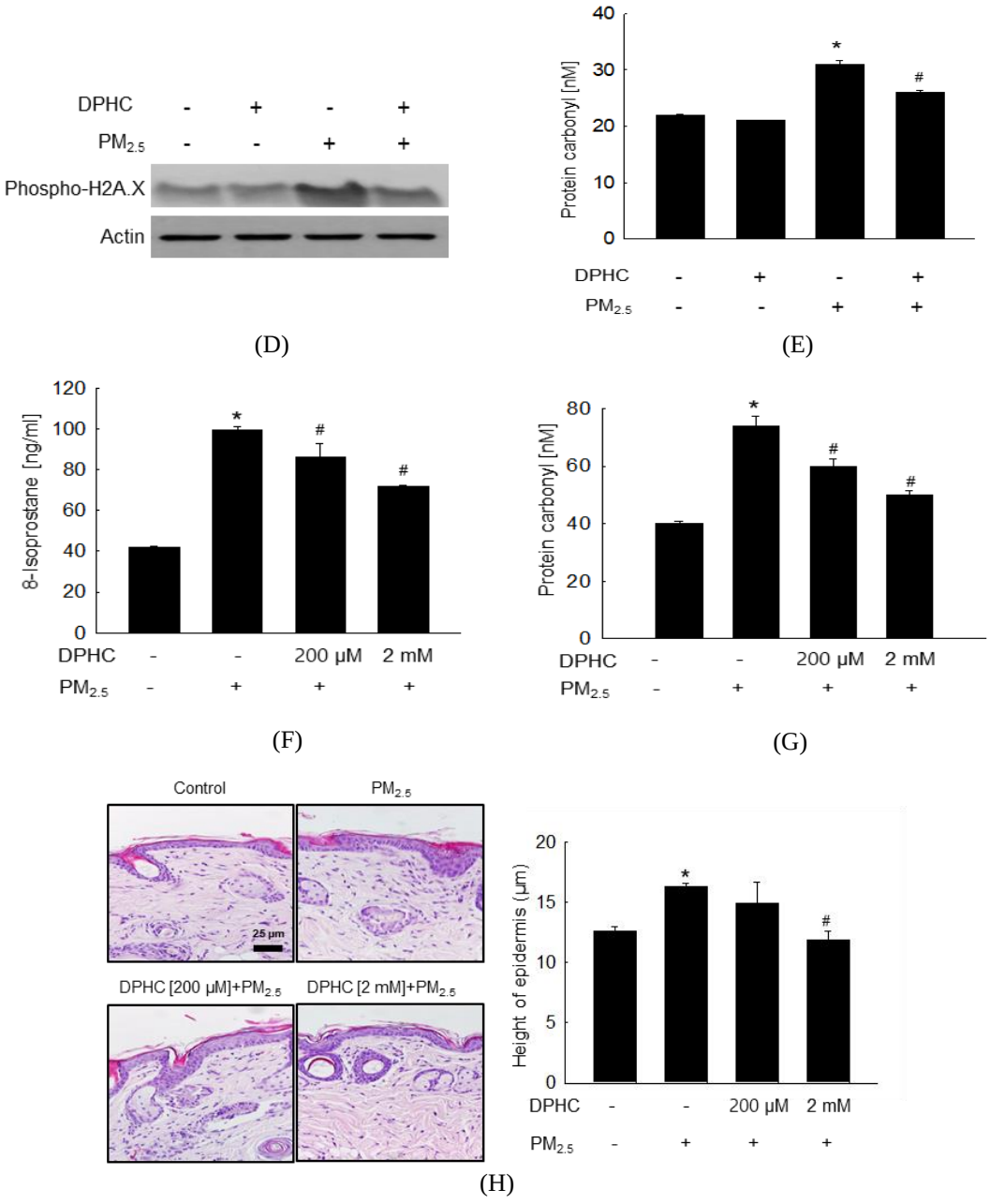

Figure 2. continued (D) Western blotting was used to determine the expression of phospho-H2A.X. (E) The protein carbonylation was examined using a protein carbonyl ELISA kit *in vitro*. (F) The protein carbonylation was examined using a protein carbonyl ELISA kit *in vivo*. (G) The lipid peroxidation was assessed *in vivo* using an 8-iso-Prostaglandin F2α ELISA kit. (H) The images of histological analysis were taken for epidermal height measurement. *$p < 0.05$ and #$p < 0.05$ vs. control and $PM_{2.5}$-treated group, respectively.

제주대학교 중앙도서관
JEJU NATIONAL UNIVERSITY LIBRARY

DPHC maintained homeostasis ER stress and autophagy under $PM_{2.5}$ exposure

ER is the main reservoir of calcium in cells, which is critical for Ca^{2+} homeostasis (Piao *et al.*, 2018). In the result, $PM_{2.5}$-exposed cells displayed a higher level of Ca^{2+}, whereas the high fluorescence intensity indicated the level of Ca^{2+} was inhibited by treatment with DPHC (Figure 3A). In addition, under ER stress, activated IRE1α promoted the transcription of CHOP, which is responsible for apoptosis (Pauly *et al.*, 2017). The proteins of phospho-IRE1α and CHOP of cells in the $PM_{2.5}$ group were increased, which were decreased by DPHC treatment (Figure 3B). Furthermore, ER stress is tightly related to the process of autophagy for activating self-degradation (Nishitoh, 2012). And the autophagy-related proteins of Beclin-1 and LC3B-II were upregulated by $PM_{2.5}$ treatment, which was reversed by DPHC (Figure 3C). In Figure 3D, $PM_{2.5}$ treatment accumulated the level of orange/red autophagic lysosomes, while DPHC minimized those cytoplasmic vesicles. Taken together, ER stress and autophagic activation induced by $PM_{2.5}$ could be suppressed by DPHC treatment.

제주대학교 중앙도서관
JEJU NATIONAL UNIVERSITY LIBRARY

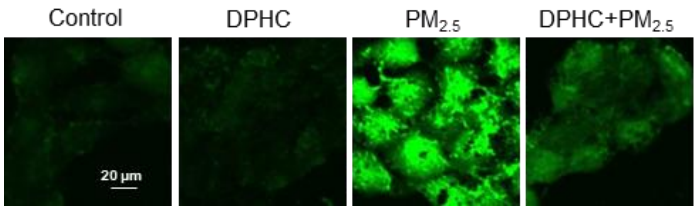

(A)

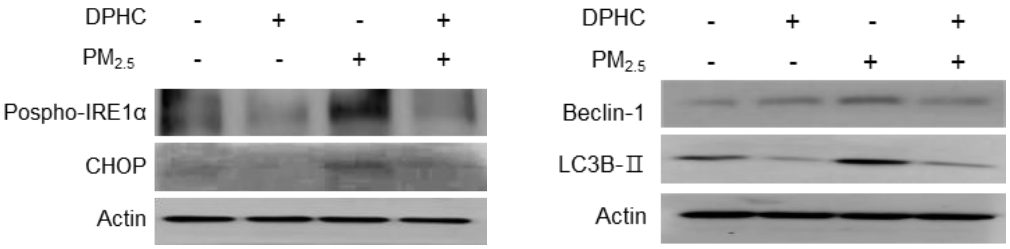

(B) (C)

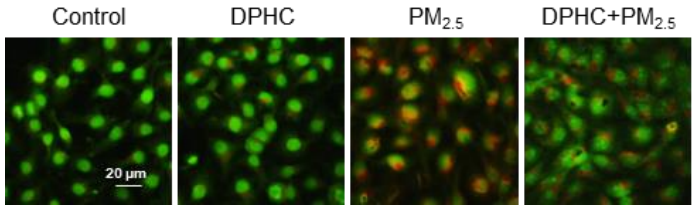

(D)

Figure 3. DPHC protected cells from $PM_{2.5}$-induced ER stress and autophagy. (A) The intracellular Ca^{2+} levels with Fluo-4 AM were assessed under confocal microscopy. (B) The protein levels of phospho-IRE1α and CHOP, and (C) Beclin-1 and LC3B-II in cell lysates were measured by western blotting. (D) The cellular acid vesicles were visualized by acridine orange staining.

제주대학교 중앙도서관
JEJU NATIONAL UNIVERSITY LIBRARY

DPHC preserved mitochondrial function under $PM_{2.5}$ exposure

ROS is one of the toxic byproducts during ATP production in mitochondria, massive of which causes mitochondrial dysfunction (Chuang *et al.*, 2020). In this result, excessive ROS in mitochondria was induced by $PM_{2.5}$ exposure, which was inhibited by DPHC treatment (Figure 4A). Similarly, the Ca^{2+} level in mitochondria induced by $PM_{2.5}$ exposure was reduced by DPHC (Figure 4B). Mitochondrial potential and permeability are highly related to caspase-mediated apoptosis (Chaudhary *et al.*, 2016). And $PM_{2.5}$ exposure caused depolarization of mitochondrial membrane potential ($\Delta\Psi m$), whereas DPHC treatment rebuilt the $\Delta\Psi m$ balance (Figure 4C, 4D). Thus, DPHC maintained cellular mitochondrial ROS level, Ca^{2+} levels, and membrane potential under $PM_{2.5}$ exposure.

제주대학교 중앙도서관
JEJU NATIONAL UNIVERSITY LIBRARY

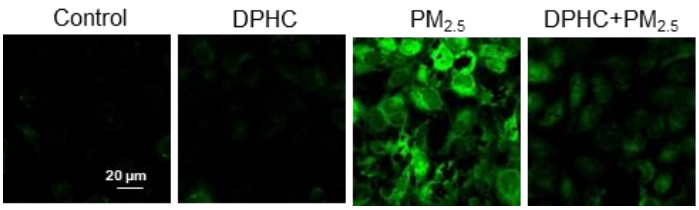

(A)

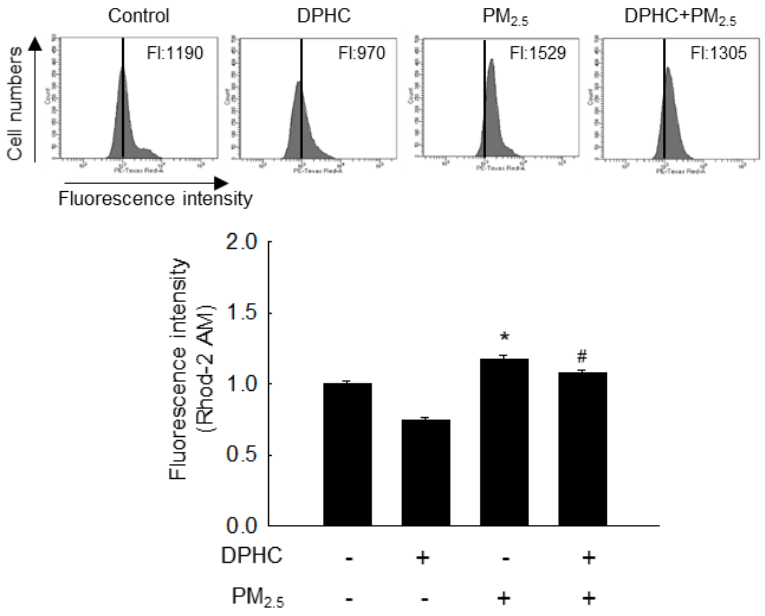

(B)

Figure 4. Mitochondrial dysfunction induced by $PM_{2.5}$ was prevented by DPHC. (A) DHR123 staining was used to detect the mitochondrial ROS with confocal microscopy. (B) Rhod-2 AM staining was used to detect the mitochondrial Ca^{2+} level by a flow cytometer. *$p < 0.05$ and #$p < 0.05$ vs. control and $PM_{2.5}$-treated group, respectively.

제주대학교 중앙도서관
JEJU NATIONAL UNIVERSITY LIBRARY

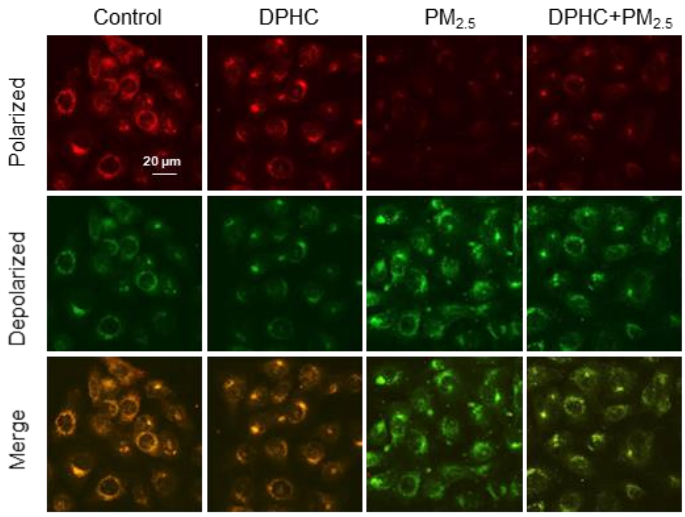

(C)

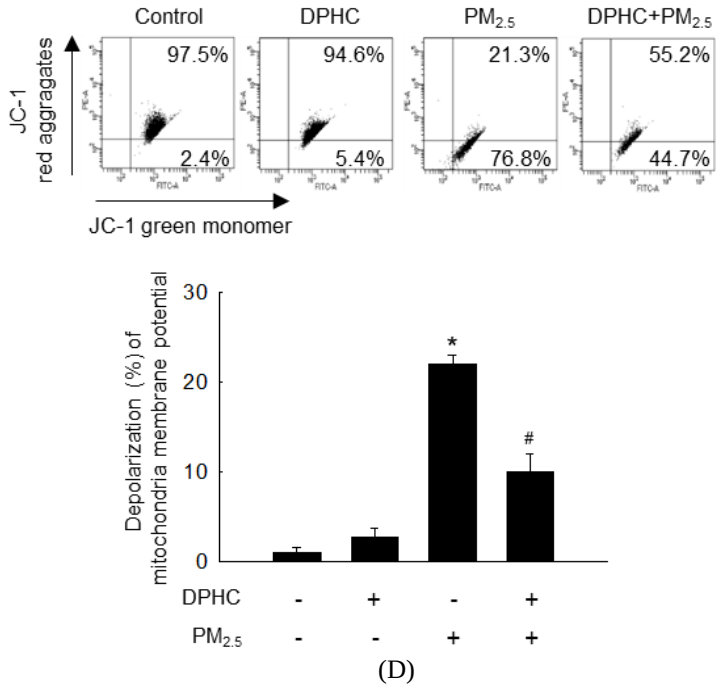

(D)

Figure 4. continued (C, D) Images and data of mitochondrial ΔΨm were obtained with JC-1 staining under confocal microscopy and flow cytometry, respectively. **p* < 0.05 and #*p* < 0.05 vs. control and $PM_{2.5}$-treated group, respectively.

제주대학교 중앙도서관
JEJU NATIONAL UNIVERSITY LIBRARY

DPHC decreased $PM_{2.5}$-induced keratinocyte apoptosis

$PM_{2.5}$ exposure inhibited the expression of the antiapoptotic protein, Bcl-2, but promoted the expression of the apoptotic protein, Bax. However, DPHC restrained the Bax level and sustained the Bcl-2 level (Figure 5A). Similarly, DPHC also restricted $PM_{2.5}$-increased active forms of caspase-9 and caspase-3 (Figure 5B). The sub-G_1 phase cell population was at a higher level in the $PM_{2.5}$ exposure group, whereas it was decreased by DPHC treatment (Figure 5C). In addition, $PM_{2.5}$ exposure caused condensed nuclei in keratinocytes, which indicated apoptosis, whereas DPHC inhibited the accumulation of apoptotic bodies (Figure 5D). What's more, Z-VAD-FMK was applied to confirm the impact of caspase activation on apoptosis. Notably, apoptotic bodies induced by $PM_{2.5}$ exposure were reduced by Z-VAD-FMK treatment, DPHC treatment, or both (Figure 5E).

제주대학교 중앙도서관
JEJU NATIONAL UNIVERSITY LIBRARY

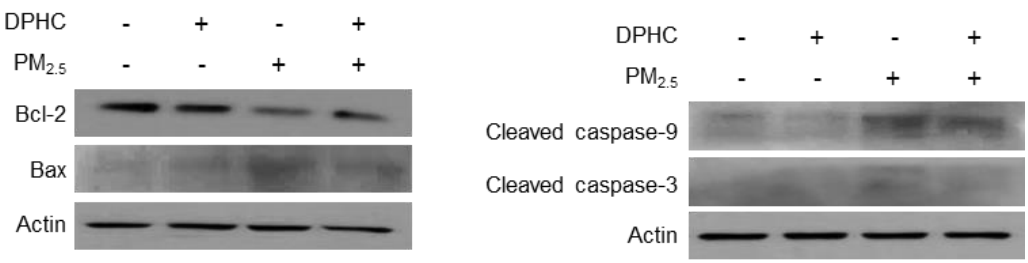

(A)

(B)

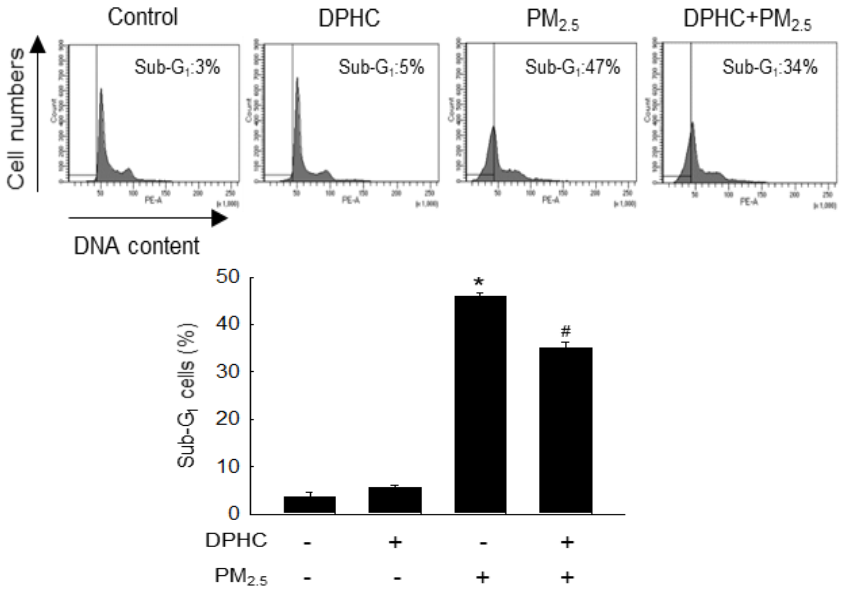

(C)

Figure 5. $PM_{2.5}$-induced cell apoptosis was limited by DPHC. (A, B) The apoptosis-related proteins of Bcl-2 and Bax, and caspase-related proteins of cleaved caspase-9 and cleaved caspase-3 in cell lysates were analyzed using western blotting. (C) Sub-G_1 populations with PI staining were measured by flow cytometry. *$p < 0.05$ and #$p < 0.05$ vs. control and $PM_{2.5}$-treated group, respectively.

제주대학교 중앙도서관
JEJU NATIONAL UNIVERSITY LIBRARY

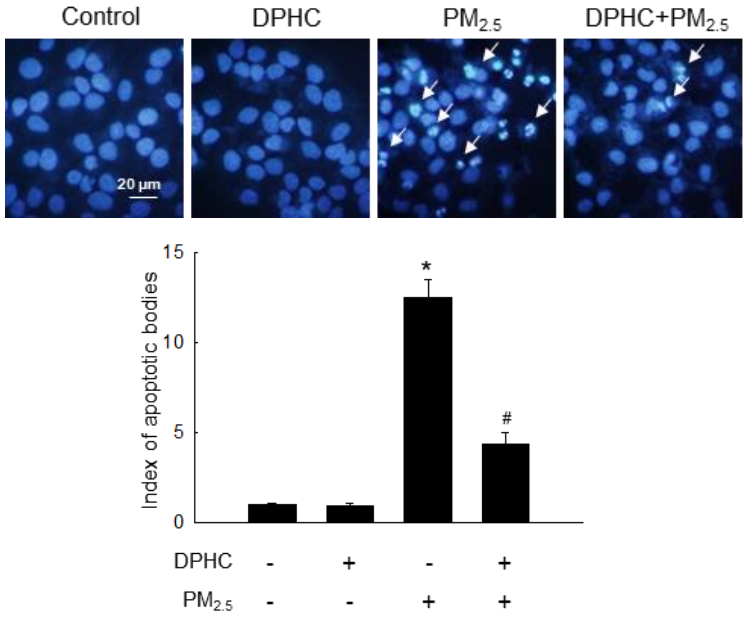

(D)

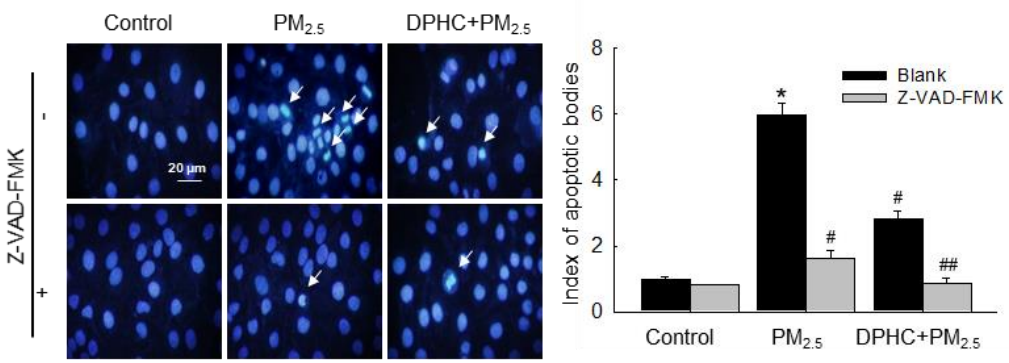

(E)

Figure 5. continued (D) Apoptotic bodies visualized by Hoechst 33342 staining; arrows indicated apoptotic bodies. (E) The formation of apoptotic cells was assessed by Hoechst 33342 staining. *$p < 0.05$, #$p < 0.05$, and ##$p < 0.05$ vs. control, $PM_{2.5}$-exposed, and DPHC-pretreated plus $PM_{2.5}$-exposed cells, respectively.

제주대학교 중앙도서관
JEJU NATIONAL UNIVERSITY LIBRARY

DPHC regulated MAPK signaling pathway to reduce $PM_{2.5}$-induced apoptotic bodies

The previous study showed that the MAPK signaling pathway is involved in cell apoptosis via the phosphorylation of ERK, p38, and JNK. The result further proved that $PM_{2.5}$ exposure induced the expression levels of phospho-ERK, phospho-p38, and phospho-JNK, which were decreased by DPHC treatment (Figure 6A). And DPHC and/or MAPK signaling-related inhibitors (U0126, SB203580, and SP600125; inhibitors of MEK (upstream of ERK), p38, and JNK, respectively) lowered the $PM_{2.5}$-induced apoptotic bodies in skin HaCaT keratinocytes (Figure 6B). Therefore, DPHC inhibited $PM_{2.5}$-induced apoptosis by inactivation of the MAPK signaling pathway.

제주대학교 중앙도서관
JEJU NATIONAL UNIVERSITY LIBRARY

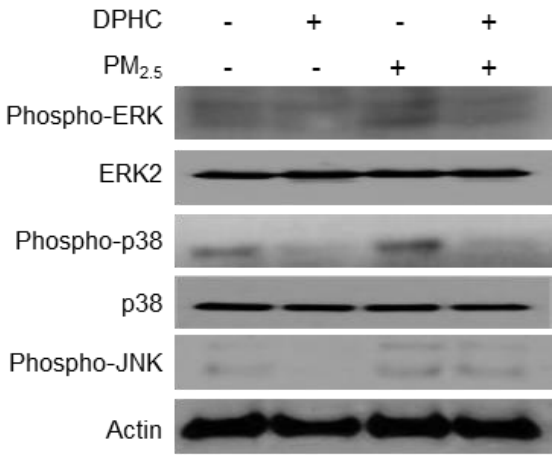

(A)

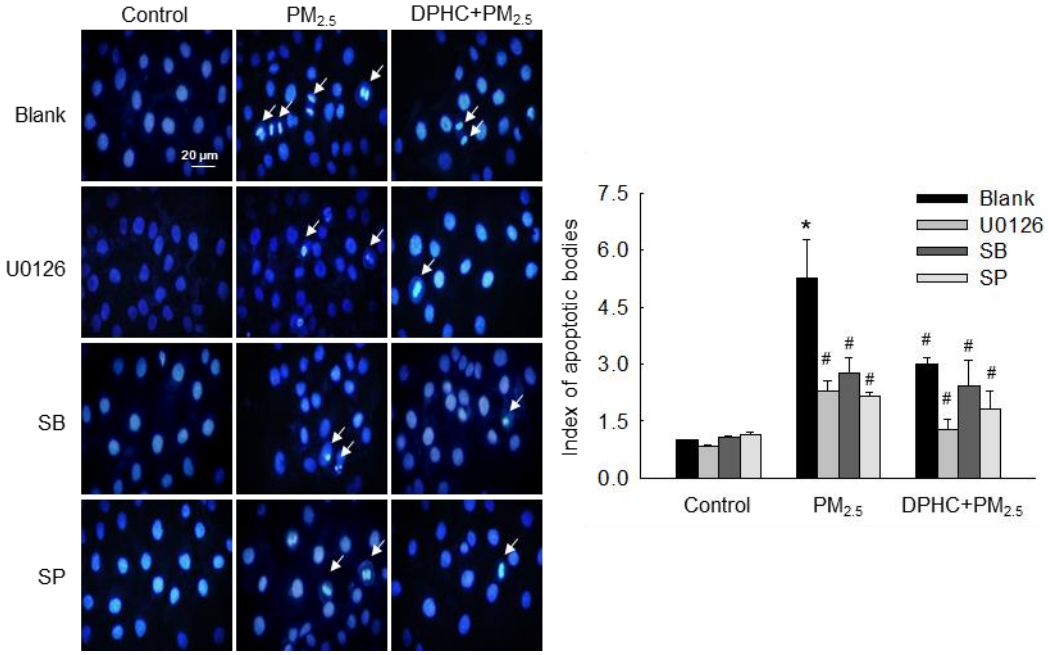

(B)

Figure 6. DPHC prevented $PM_{2.5}$-exposed cell apoptosis via the MAPK signaling pathway. (A) Cell lysates were analyzed to detect phosphorylation of ERK, p38, and JNK using western blotting. (B) Analysis of Hoechst 33342-stained apoptotic cells, after treatment with U0126, SB203580 (SB), and SP600125 (SP), which are inhibitors of MEK, p38, and JNK, respectively; $*p < 0.05$ and $\#p < 0.05$ compared with control and $PM_{2.5}$-exposed cells, respectively.

제주대학교 중앙도서관
JEJU NATIONAL UNIVERSITY LIBRARY

DISCUSSION

Previous studies showed that DPHC suppressed ROS generation further blocking MMP-1 expression (Piao *et al.*, 2015a), and activating the nucleotide excision repair system to inhibit UVB-induced DNA damage in human HaCaT cells (Piao *et al.*, 2015b). Studies have also shown that $PM_{2.5}$ may penetrate the skin barrier and damage the keratinocytes (Krutmann *et al.*, 2014; Li *et al.*, 2017). Therefore, I tested the protective effects of DPHC on $PM_{2.5}$-induced skin damage in this study. DPHC, as a phlorotannin, showed no cytotoxicity to human HaCaT cells from 2.5 to 40 μM and showed radical scavenging activity in the DPPH assay. Furthermore, the results showed that there was no significant difference in the DPPH scavenging effect between concentrations of 20 and 40 μM. In addition, our previous studies showed that DPHC inhibited both superoxide anions and hydroxyl radicals directly at 20 μM (Piao *et al.*, 2013). Therefore, I used DPHC at 20 μM as the test concentration in the subsequent experiments. A recent study demonstrated that $PM_{2.5}$ changed the morphology of keratinocytes because of ROS overproduction, which damages the intracellular antioxidant system (Hu *et al.*, 2017). Therefore, I investigated $PM_{2.5}$-induced intracellular ROS production in keratinocytes and the results showed that $PM_{2.5}$ promoted ROS generation, lowered cell viability, and damaged cell structures such as DNA by inducing lipid peroxidation. However, DPHC blocked intracellular ROS generation, increased cell viability, and protected the cell structure. *In vivo* experiments also proved that the oxidation of polyunsaturated fatty acids and the protein carbonylation as well as epidermal height were increased by $PM_{2.5}$; however, the generations of these two substances and the increase of epidermal height were inhibited by DPHC.

ER stress plays a crucial role in intracellular dysfunction and may be induced by $PM_{2.5}$ (Piao *et al.*, 2018). In ER transmembrane proteins regulation, GRP78 facilitates misfolded protein refolding of mainly PERK, IRE1α, and ATF6 (Mei *et al.*, 2013). These results showed that DPHC suppressed $PM_{2.5}$-induced ER stress, and balanced Ca^{2+} dynamics, which was

제주대학교 중앙도서관
JEJU NATIONAL UNIVERSITY LIBRARY

essential to ER function. In addition, $PM_{2.5}$ induced the phosphorylation of IRE1α and upregulated protein levels of GRP78 and CHOP, which indicated that $PM_{2.5}$ activated the ER stress pathway in HaCaT cells. Furthermore, these effects were reversed by DPHC. A previous review reported that ER stress may induce cell death through autophagy (Sano *et al.*, 2013). In the autophagic process, various ATGs including ATG5, Beclin-1, and the microtubule-associated protein LC3B play a very important role. Beclin-1 is involved in the nucleation of the phagophore and autophagosome formation (Shrestha *et al.*, 2018). Therefore, the protein levels of Beclin-1and LC3-II were detected, which were increased by $PM_{2.5}$; however, DPHC decreased this effect.

In addition to ER stress, mitochondrial dysfunction is related to intracellular ROS generation and causes cell damage. Previous studies proved that elevated ROS levels induced by UVA irradiation also decrease the ΔΨm, which induces the generation of cytochrome C and apoptosis-related factors (Xin *et al.*, 2021). Our results demonstrated that $PM_{2.5}$ induced mitochondrial ROS generation and caused mitochondrial swelling. In addition, $PM_{2.5}$ promoted the protein level of Bax, which is an apoptosis-related protein, and blocked that of Bcl-2, an anti-apoptotic protein. However, DPHC reversed all these effects, suggesting that it protected cells against $PM_{2.5}$-induced mitochondria damage.

Because $PM_{2.5}$ may be related to cell apoptosis, I examined nuclear condensation, which is one of the characteristics of apoptotic cells. The result showed that $PM_{2.5}$ promoted the development of apoptotic bodies and activated caspases-3 and -9, two key apoptotic proteins. However, DPHC inhibited cell apoptosis, which suggested that it protected the cells from apoptosis by regulating the levels of apoptosis-associated proteins.

Previously, the MAPK signaling pathway was shown to degrade Bcl-2 and activate Bax, resulting in mitochondrial-mediated apoptotic cell death (Tang *et al.*, 2021). Therefore, I detected the expression levels of the MAPK signaling-associated proteins. Phosphorylation of ERK, p38, and JNK was upregulated by $PM_{2.5}$ and downregulated by DPHC pretreatment. The

제주대학교 중앙도서관
JEJU NATIONAL UNIVERSITY LIBRARY

effects of MAPK signaling were further explored using MEK, p38, and JNK inhibitors. DPHC pretreatment reduced apoptotic cell number, and MAPK signaling-related inhibitors also contributed to reducing the number of apoptotic bodies, which indicated that DPHC may inhibit cell death through the MAPK signaling pathway.

제주대학교 중앙도서관
JEJU NATIONAL UNIVERSITY LIBRARY

PART II

Eckol Protected Skin Keratinocyte Damage from Particulate Matter via MAPK Signaling Pathway

This work has been published as titled “Eckol Inhibits Particulate Matter 2.5-Induced Skin Keratinocyte Damage via MAPK Signaling Pathway” in Marine Drugs (2019;17:444).

제주대학교 중앙도서관
JEJU NATIONAL UNIVERSITY LIBRARY

ABSTRACT

The toxicity of particulate matter towards the epidermis has been well-established in many epidemiological studies; it is manifested in various forms, including cancer, aging, and skin loss. In this study, it aimed to show the mechanism underlying the protective effects of eckol, a phlorotannin isolated from brown seaweed, towards human HaCaT keratinocytes from $PM_{2.5}$-induced cell death. First, to elucidate the underlying mechanism of toxicity of $PM_{2.5}$, I checked the ROS level, which contributed significantly to cell damage. Experimental data indicated that excessive ROS caused damage to lipids, proteins, and DNA and induced mitochondrial dysfunction. Furthermore, eckol decreased ROS generation, ensuring the stability of molecules, and maintaining a steady mitochondrial state. The western blot analysis showed that $PM_{2.5}$ promoted apoptosis-related protein levels and activated MAPK signaling pathway, whereas eckol protected cells from apoptosis by inhibiting MAPK signaling pathway. This was further reinforced by detailed investigations using MAPK inhibitors. Thus, our results demonstrated that inhibition of $PM_{2.5}$-induced cell apoptosis by eckol was through the MAPK signaling pathway.

KEYWORDS

Eckol, particulate matter 2.5; oxidative stress; human HaCaT keratinocytes

제주대학교 중앙도서관
JEJU NATIONAL UNIVERSITY LIBRARY

INTRODUCTION

Natural compounds could be effective candidates for various skin diseases. Particularly, phlorotannin extracted from seaweeds has interesting properties that make them useful for cosmeceutical applications. It could whiten the skin by inhibiting melanin synthesis (Kim *et al.*, 2019), and adjust macrophages by inhibiting inflammatory profile (Kong *et al.*, 2011). Moreover, phlorotannin shows antioxidant (Gheda *et al.*, 2021), anti-inflammatory (Sanjeewa *et al.*, 2016), and hair-growth promotion activities (Chang *et al.*, 2016). Studies have shown that eckol, which is a kind of phlorotannin present in brown seaweeds, decreases the oxidative stress in human keratinocytes (Piao *et al.*, 2012), inhibits cancer (Monteiro *et al.*, 2022), and declines the inflammatory index in HaCaT keratinocytes (Cho *et al.*, 2020). Our earlier studies have proved that eckol could clear excess ROS and protect skin keratinocytes from apoptosis (Piao *et al.*, 2012).

Air pollution by the continuous emission of various pollutants into the atmosphere has accelerated climate change and modernization (Kim *et al.*, 2013). According to previous studies, PM increases the public health risks for various diseases, such as respiratory disease (Wu *et al.*, 2021), cardiovascular disease (Ain & Qamar, 2021), and lung development (Lim & Yoon, 2022). Fine particulate matter with a diameter of less than 2.5 μm, denoted as $PM_{2.5}$. Significantly, $PM_{2.5}$ could deeply penetrate the skin and the respiratory tract (Kim *et al.*, 2015). Skin damage caused by $PM_{2.5}$ is manifested as inflammatory skin diseases, such as atopic dermatitis, acne, psoriasis, aging, and cancer via multiple signaling pathways (Kim *et al.*, 2016). Based on this evidence of its protective action, I was interested to unravel the mechanism underlying the protective action of eckol on $PM_{2.5}$-induced skin cell apoptosis.

제주대학교 중앙도서관
JEJU NATIONAL UNIVERSITY LIBRARY

RESULTS

Eckol inhibited cell damage via the reduction of oxidative stress

Previous studies have shown that eckol exhibited no cytotoxicity to HaCaT cells up to 50 μM (Kang *et al.*, 2015b), but showed antioxidant activity (Piao *et al.*, 2012). Therefore, I used 30 μM of eckol as the optimal concentration in this study. Although $PM_{2.5}$ increased the levels of ROS, eckol inhibited intracellular ROS generation (Figure 7A, 7B). The results demonstrated that $PM_{2.5}$-induced ROS could accelerate cell apoptosis and death. To confirm that eckol could help cells escape from this damage, I checked cell arrest, nuclei integrity, and cell viability. According to the results, $PM_{2.5}$ treatment led to apoptosis including high levels of sub-G_1 cell phase (Figure 7C) and fragmented nuclei (Figure 7D). However, it was noted that following treatment with eckol, the percentage of cells with a normal cell cycle was increased, and the number of apoptotic bodies was decreased. Therefore, eckol could protect keratinocytes from $PM_{2.5}$-induced cell cycle arrest and apoptosis by inhibiting ROS generation.

제주대학교 중앙도서관
JEJU NATIONAL UNIVERSITY LIBRARY

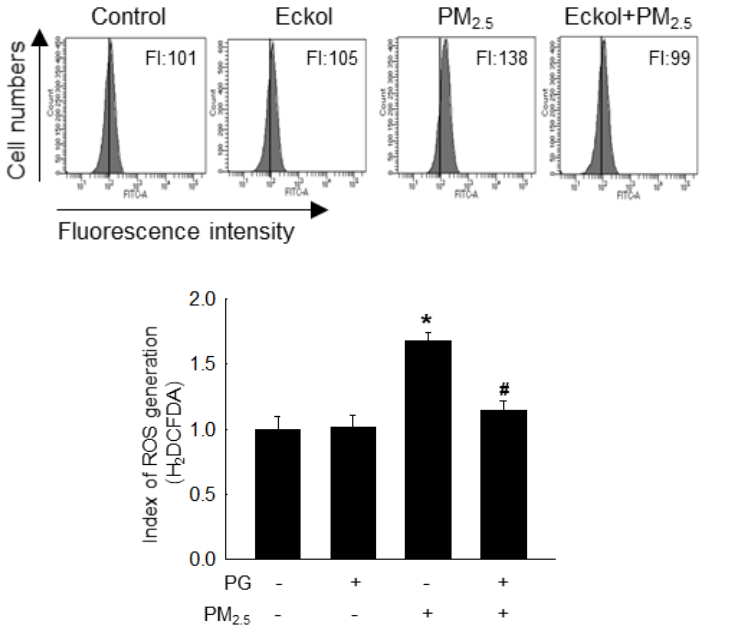

(A)

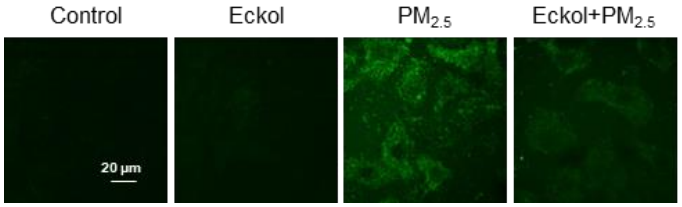

(B)

Figure 7. Eckol decreased cell apoptotic bodies by inhibiting $PM_{2.5}$-induced ROS levels. Intracellular ROS level (H_2DCFDA staining) induced by $PM_{2.5}$ (50 μg/mL) was inhibited via treatment with eckol (30 μM) as observed by (A) flow cytometry and (B) confocal microscope. *$p < 0.05$ and #$p < 0.05$ vs. control cells and $PM_{2.5}$-exposed cells, respectively.

제주대학교 중앙도서관
JEJU NATIONAL UNIVERSITY LIBRARY

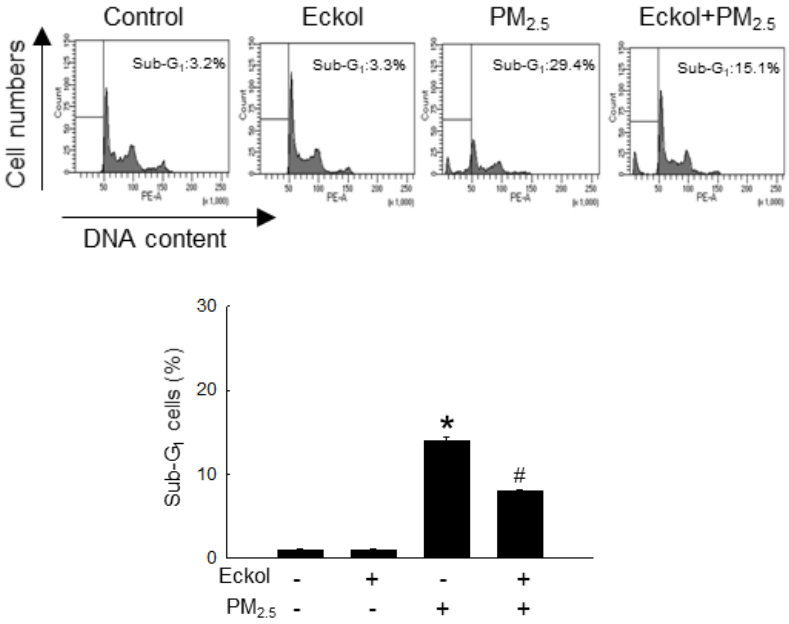

(C)

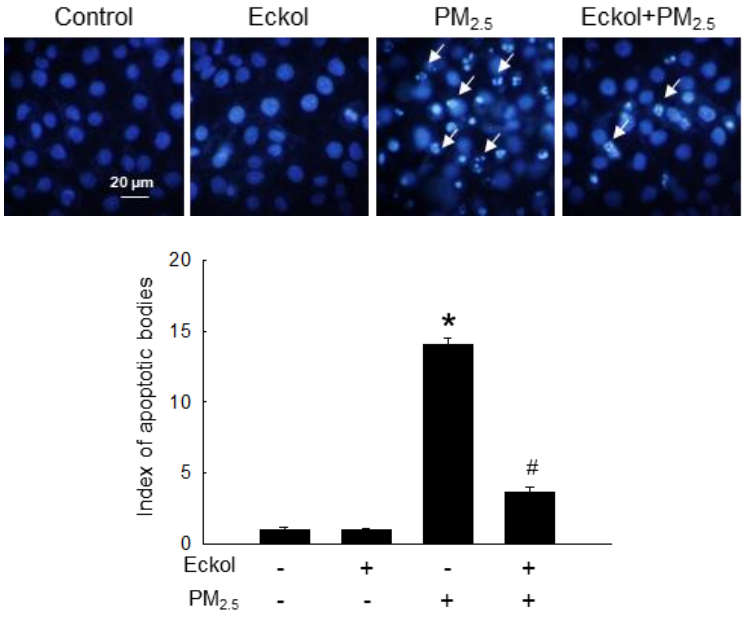

(D)

Figure 7. continued (C) Sub-G_1 cell cycle arrest induced by $PM_{2.5}$ was blocked by treatment with eckol, as determined by PI staining. (D) Apoptosis induced by $PM_{2.5}$ was reduced by treatment with eckol, observed by Hoechst 33342 staining. *$p <$ 0.05 and #$p < 0.05$ vs. control cells and $PM_{2.5}$-exposed cells, respectively.

제주대학교 중앙도서관
JEJU NATIONAL UNIVERSITY LIBRARY

Eckol ameliorated $PM_{2.5}$-induced macromolecular damage

Previous studies have shown that an increment in ROS disrupted intracellular molecules involved in apoptosis (Hyun *et al.*, 2019; Ghosh *et al.*,2012); next, I detected lipid peroxidation, protein carbonylation, and DNA damage. The confocal images showed that $PM_{2.5}$ caused the generation of phosphine oxide, which is a marker of lipid peroxidation. However, this was reversed by treatment with eckol (Figure 8A). Moreover, $PM_{2.5}$ aggravated protein carbonylation level, which was decreased by eckol treatment (Figure 8B). DNA lesions and strand breaks were studied by staining the cells with avidin-TRITC (Figure 8C) and comet assay (Figure 8D). The data showed that eckol guarded DNA against $PM_{2.5}$. From these results, eckol protected cells from $PM_{2.5}$-induced macromolecular damage.

제주대학교 중앙도서관
JEJU NATIONAL UNIVERSITY LIBRARY

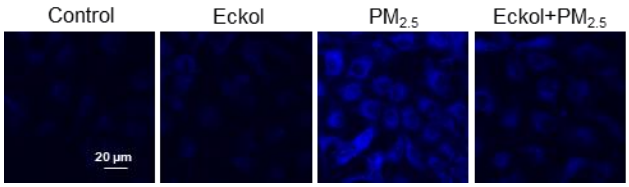

(A)

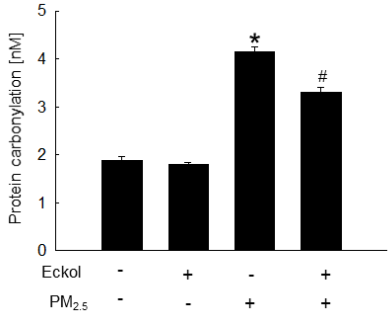

(B)

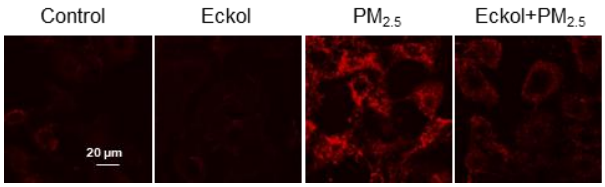

(C)

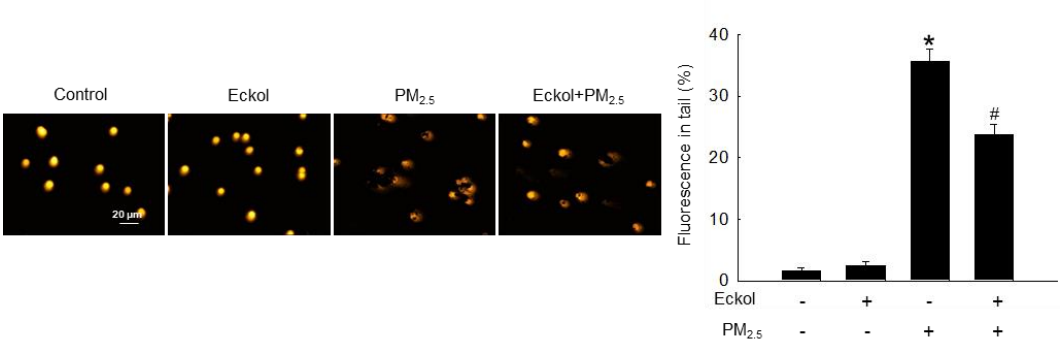

(D)

Figure 8. Eckol protected cellular molecules from $PM_{2.5}$-induced damage. (A) Lipid oxidation induced by $PM_{2.5}$ was mitigated via treatment with eckol through DPPP staining. (B) Protein carbonylation induced by $PM_{2.5}$ was declined via treatment with eckol as observed by a protein carbonylation assay. DNA damage induced by $PM_{2.5}$ was inhibited via treatment with eckol, as confirmed through (C) avidin-TRITC staining and (D) comet assay. *$p < 0.05$ and #$p < 0.05$ vs. control cells and $PM_{2.5}$-exposed cells, respectively.

제주대학교 중앙도서관
JEJU NATIONAL UNIVERSITY LIBRARY

Eckol prevented $PM_{2.5}$-induced mitochondrial dysfunction

Mitochondria play an important role in cellular energy production, and their biogenesis is related to the synthesis of molecules, such as lipids and proteins, DNA transcription, and even cell apoptosis (Shin *et al.*, 2017). Next, I examined mitochondrial functions. DHR123 staining images showed that mitochondrial ROS was accumulated in the $PM_{2.5}$-treated group; whereas ROS level was decreased by pretreatment with eckol (Figure 9A). Both flow cytometry (Figure 9B) and confocal microscopy (Figure 9C) data demonstrated that $PM_{2.5}$ caused mitochondrial depolarization, which was arrested by treatment with eckol. Furthermore, the flux of intracellular calcium was increased in the $PM_{2.5}$-treatment group, and it was decreased in the eckol-treatment group, which was monitored using the calcium indicator, Rhod-2 AM, by confocal microscopy (Figure 9D) and flow cytometry (Figure 9E). All these data suggested that $PM_{2.5}$ induced disordered mitochondrial functions, which was prevented by eckol.

제주대학교 중앙도서관
JEJU NATIONAL UNIVERSITY LIBRARY

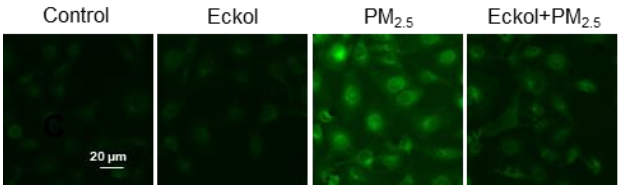

(A)

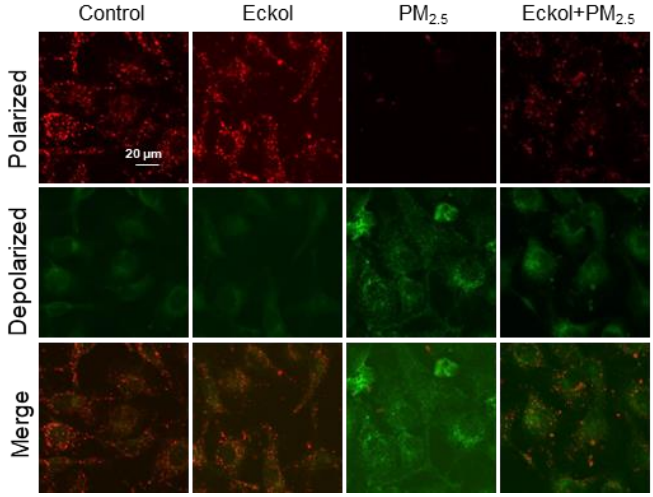

(B)

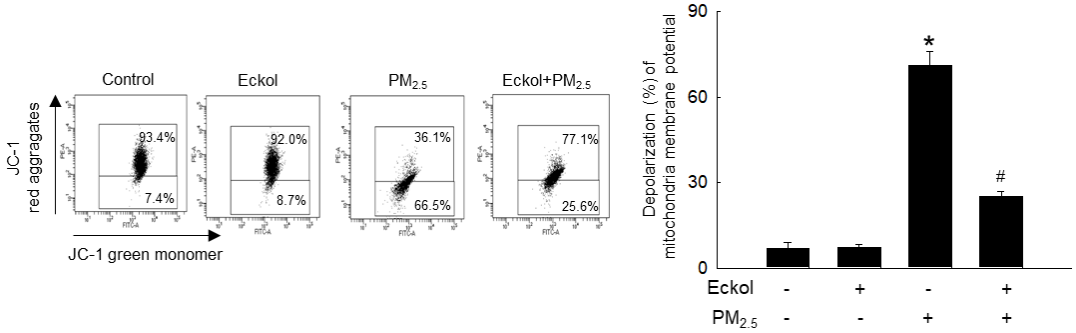

(C)

Figure 9. Eckol prevented $PM_{2.5}$-induced mitochondrial dysfunction by balancing calcium level and mitochondrial membrane potential. (A) Mitochondrial ROS induced by $PM_{2.5}$ was decreased via treatment with eckol through DHR123 staining. Depolarization of mitochondrial membrane potential (JC-1 staining) induced by $PM_{2.5}$ was repolarized via treatment with eckol through (B) confocal microscopy and (C) flow cytometry. *$p < 0.05$ and #$p < 0.05$ vs. control cells and $PM_{2.5}$-exposed cells, respectively.

제주대학교 중앙도서관
JEJU NATIONAL UNIVERSITY LIBRARY

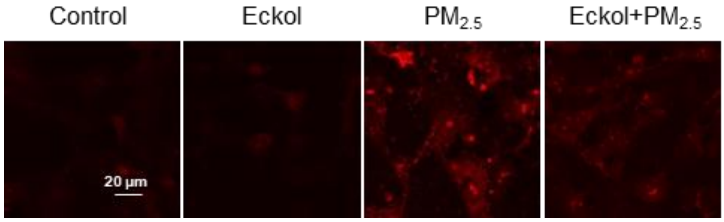

(D)

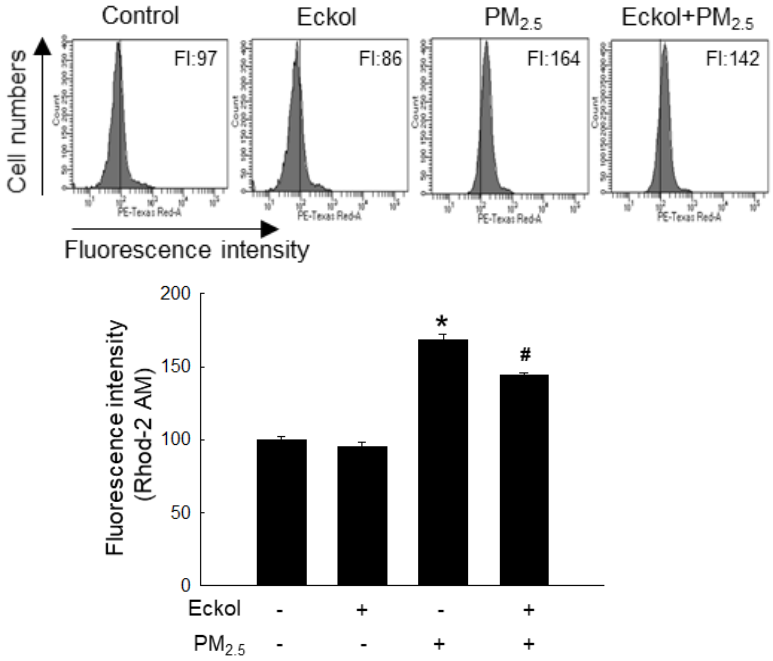

(E)

Figure 9. continued Extra-mitochondrial Ca^{2+} (Rhod-2 AM staining) induced by $PM_{2.5}$ was blocked by treatment with eckol and was monitored using (D) confocal microscopy and (E) flow cytometry. *$p < 0.05$ and #$p < 0.05$ vs. control cells and $PM_{2.5}$-exposed cells, respectively.

제주대학교 중앙도서관
JEJU NATIONAL UNIVERSITY LIBRARY

Eckol restrained $PM_{2.5}$-induced apoptosis

It has been reported that urban particulate pollution penetrates the skin barrier and causes apoptosis in keratinocytes by activating caspase-3 (Pan *et al.*, 2015). Therefore, I evaluated the levels of the anti-apoptosis protein Bcl-2, the proapoptotic protein Bax, and cleaved caspase-3 (Figure 10A). The protein levels of activated caspase-3 and Bax were increased by $PM_{2.5}$, but an expression of Bcl-2 was decreased by treatment with $PM_{2.5}$; however, these were reversed by eckol treatment. To investigate whether $PM_{2.5}$ could induce apoptosis, I counted apoptotic bodies via Hoechst 33342 staining (Figure 10B). The index of apoptotic cells in the $PM_{2.5}$ group surged four times compared to that in the control group; however, both eckol and Z-VAD-FMK (the caspase inhibitor) halted the apoptotic bodies induced by $PM_{2.5}$. Thus, eckol inhibited apoptosis induced by $PM_{2.5}$ through the inactivation of caspase-3.

제주대학교 중앙도서관
JEJU NATIONAL UNIVERSITY LIBRARY

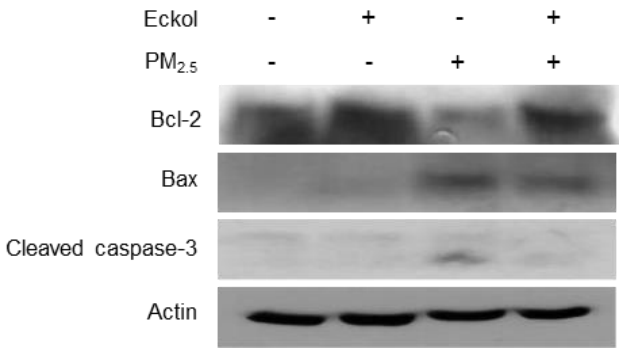

(A)

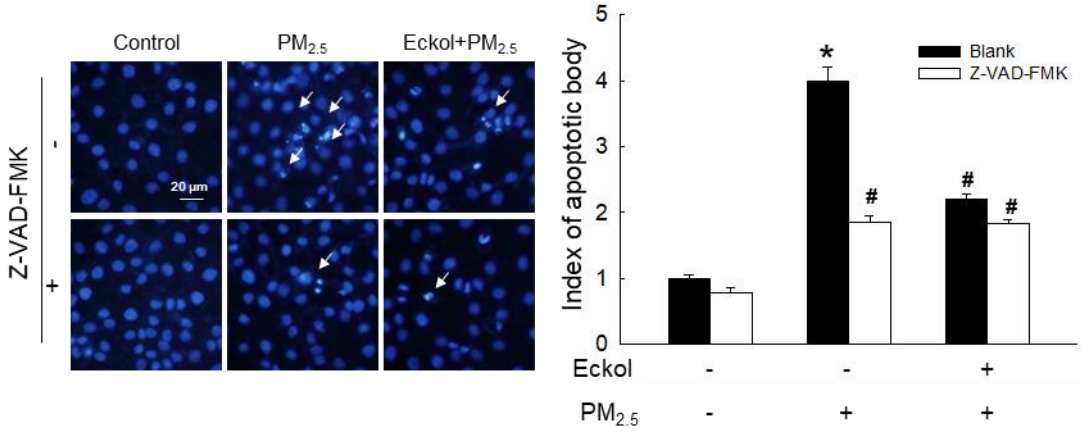

(B)

Figure 10. Eckol reduced $PM_{2.5}$-induced apoptotic bodies by regulating apoptosis-related proteins. (A) The protein levels of Bcl-2, Bax and cleaved caspase-3 were observed by western blotting. (B) Apoptosis was detected by Hoechst 33342 staining. *$p < 0.05$ and #$p < 0.05$ vs. control cells and $PM_{2.5}$-exposed cells, respectively.

제주대학교 중앙도서관
JEJU NATIONAL UNIVERSITY LIBRARY

Eckol reduced $PM_{2.5}$-induced apoptosis by inactivating MAPK signaling pathway

In a review, Sun *et al.*, point out that many anti-cancer therapeutics induced apoptosis by inactivating the MAPK/ERK signaling pathway (Sun *et al.*, 2015). Thus, I checked expression levels of MAPK-related proteins, ERK, p38, and JNK, and the results showed that $PM_{2.5}$ could stimulate ERK, p38, and JNK (Figure 11A). However, eckol inhibited the activation of ERK, p38, and JNK. Next, I examined $PM_{2.5}$-induced apoptotic bodies by treatment with MAPK pathway inhibitors, U0126, SB203580, and SP600125 (inhibitors of MEK, p38, and JNK, respectively), and the results showed that all these three inhibitors could reduce the number of apoptotic bodies (Figure 11B). In addition, eckol enhanced the anti-apoptotic effect of MAPK-related inhibitors. Therefore, eckol inactivated MAPK signaling pathway to increase cell survival.

제주대학교 중앙도서관
JEJU NATIONAL UNIVERSITY LIBRARY

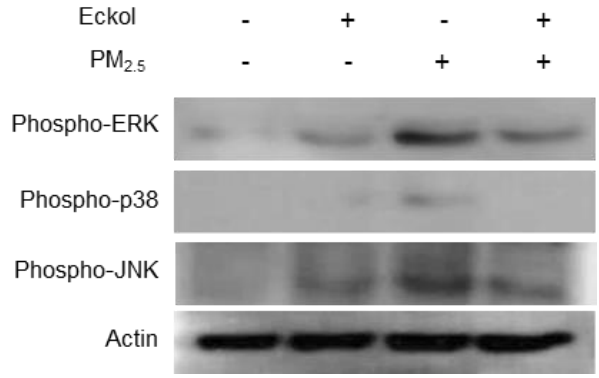

(A)

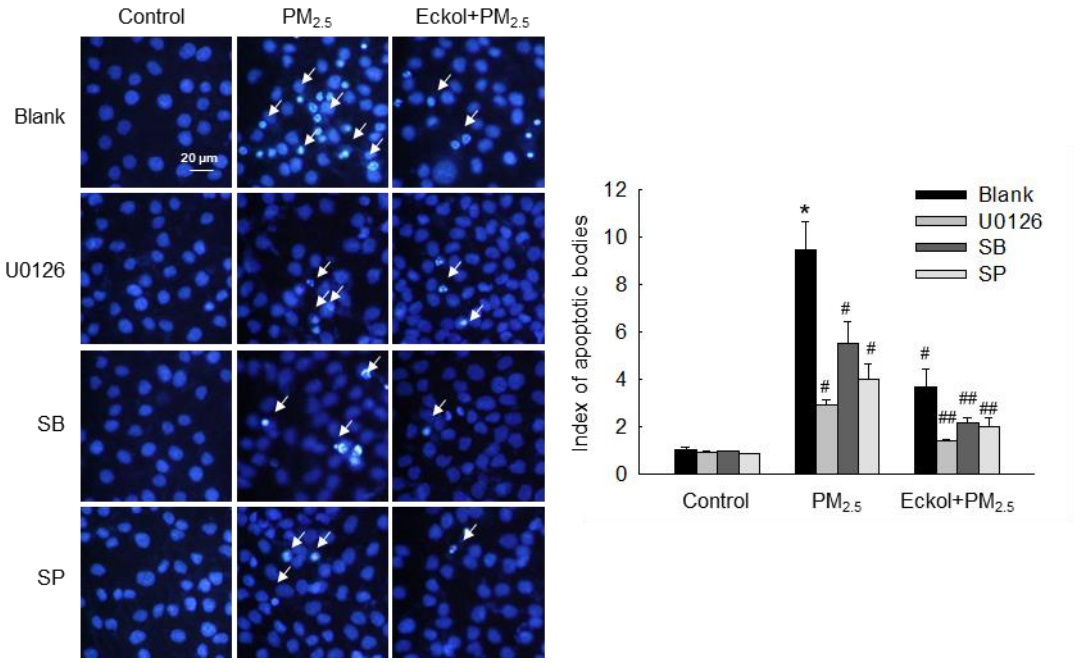

(B)

Figure 11. Eckol reduced $PM_{2.5}$-induced apoptotic bodies by inactivating MAPK signaling pathway. (A) Western blot showing that activation of ERK, p38, and JNK induced by $PM_{2.5}$ was reversed via treatment with eckol. (B) Apoptosis induced by $PM_{2.5}$ was reduced by treatment with eckol or MEK, p38, and JNK inhibitors (U0126, SB203580 (SB), and SP600125 (SP), respectively), as observed through Hoechst 33342 staining. *$p < 0.05$, #$p < 0.05$ and ##$p < 0.05$ vs. control cells, $PM_{2.5}$-exposed cells, and both eckol and $PM_{2.5}$-exposed cells respectively.

제주대학교 중앙도서관
JEJU NATIONAL UNIVERSITY LIBRARY

DISCUSSION

There have been several investigations into the bioactivities of eckol, since it was first isolated from *Ecklonia cava* (Cho *et al.*, 2020). Eckol has multi-protective effects on several cell lines, including lung fibroblast cells (Kim *et al.*, 2010), human dermal fibroblasts (Joe *et al.*, 2006), Chang liver cells (Kim *et al.*, 2014), and human keratinocytes (Piao *et al.*, 2012). Furthermore, eckol is a compound with therapeutic potential in many areas, such as anti-oxidative stress (Gheda *et al.*, 2021), radioprotective action (Park *et al.*, 2008), and anticancer activity (Monteiro *et al.*, 2022). According to a study, $PM_{2.5}$ causes cell apoptosis by generating ROS (Piao *et al.*, 2018). Usually, oxidative stress is caused by excessive accumulation of ROS or lack of the ability to eliminate them. $PM_{2.5}$ produces large amounts of ROS beyond the clearance ability of cells (Zhen *et al.*, 2019b). In our study, eckol showed its ability to protect cells against $PM_{2.5}$-induced ROS, cell cycle arrest, and apoptosis, and improved cell viability.

To explore the mechanism in detail, I checked the state of molecules such as lipids, proteins, and DNA, which play various important roles in the cells (Zhen *et al.*, 2019a). Furthermore, macromolecular damage can be recognized as oxidative stress (Trachana *et al.*, 2017). Our results demonstrated that $PM_{2.5}$ indeed induced the oxidation of molecules, whereas eckol relieved molecular damage. The mitochondria-dependent ROS generation subsequently caused cell cycle arrest and apoptosis, which is ROS-mediated apoptosis via mitochondrial mechanism (Kiang & Olabisi, 2019). In addition, our previous studies showed that calcium level and mitochondrial membrane potential affect the function of mitochondria (Piao *et al.*, 2018; Zhen *et al.*, 2019b; Zhen *et al.*, 2019c). The data in Figure 9 illustrated that $PM_{2.5}$ increased the calcium level and depolarized mitochondrial membrane potential as compared to the control cells, whereas eckol regulated the mitochondria and maintained a stable state. The mechanism of mitochondrial damage is related to Bcl-2 proteins, which maintain mitochondrial membrane integrity (Zheng *et al.*, 2016). The interaction between Bcl-2 and Bax also influences antiapoptosis (Moldoveanu *et al.*, 2014). Bcl-2 plays an anti-

제주대학교 중앙도서관
JEJU NATIONAL UNIVERSITY LIBRARY

apoptotic role, whereas Bax is proapoptotic (Czabotar *et al.*, 2014). There is a complex crosslink between Bcl family proteins and caspase proteins in cell apoptosis, in which Bcl-2 indirectly activates the caspase cascade (Gupta *et al.*, 2021). The caspase-3 results in apoptosis induced by both extrinsic and intrinsic stimuli (Asweto *et al.*, 2017). The results elucidated that except for the decrease of Bcl-2, Bax and activated caspase-3 were increased by $PM_{2.5}$; however, eckol reversed these effects. Then, I treated cells with a caspase inhibitor (Z-VAD-FMK) and found that upon pretreatment with caspase inhibitors, the apoptotic bodies were decreased significantly. These data proved that caspase proteins contributed to cell apoptosis induced by $PM_{2.5}$. MAPK signaling pathway plays a role in many systems of cell proliferation, migration, and apoptosis (Sun *et al.*, 2015). Many drugs are used to modulate MAPK signaling pathways to induce cell apoptosis in cells, such as lung cancer (Jeanson *et al.*, 2019), human colorectal cancer (Pan *et al.*, 2019), and cervical cancer HeLa cells (Yao *et al.*, 2019). Finally, I checked MAPK signaling pathway-related proteins, ERK, p38, and JNK. The results showed that $PM_{2.5}$ activated all three proteins, but eckol exhibited the ability to inactivate them. When I used inhibitors of MEK, p38, and JNK to treat $PM_{2.5}$-damaged cells, the numbers of apoptotic bodies were decreased similar to eckol. These data further proved that the MAPK signaling pathway plays a vital role in the inhibition of $PM_{2.5}$-induced apoptosis by eckol.

제주대학교 중앙도서관
JEJU NATIONAL UNIVERSITY LIBRARY

PART III

Purpurogallin Prevented Particulate Matter- and/or Ultraviolet B-Induced Skin Cell Damage

This work has been published as titled “Purpurogallin Protects Keratinocytes from Damage and Apoptosis Induced by Ultraviolet B Radiation and Particulate Matter 2.5” in Biomolecules & Therapeutics (2019;27:395-403).

제주대학교 중앙도서관
JEJU NATIONAL UNIVERSITY LIBRARY

ABSTRACT

Purpurogallin, a natural phenol obtainable from oak nutgalls, has shown antioxidant, antiproliferative, and anti-inflammatory effects. Recently, in addition to UVB radiation inducing cell apoptosis via oxidative stress, $PM_{2.5}$ was shown to trigger excessive production of reactive oxygen species. According to the study, UVB radiation and $PM_{2.5}$ synergistically damaged human HaCaT keratinocytes, leading to disrupted cellular DNA, lipids, and mitochondrial depolarization. Purpurogallin protected HaCaT cells against apoptosis which was induced by UVB radiation and/or $PM_{2.5}$. These results indicate that purpurogallin possesses antioxidant effects and protects cells from damage and apoptosis induced by UVB radiation and $PM_{2.5}$.

KEYWORDS

Purpurogallin; $PM_{2.5}$; oxidative stress; UVB; human HaCaT keratinocytes

제주대학교 중앙도서관
JEJU NATIONAL UNIVERSITY LIBRARY

INTRODUCTION

Recently, alongside UVB, $PM_{2.5}$ has become the focus of public health research, including research on skin hazards. $PM_{2.5}$ represents outdoor air pollution and mainly consists of metals, allergens, toxic products from the combustion of fossil fuels, and endotoxins (He *et al.*, 2016). PM was shown to damage the nervous system (Wang *et al.*, 2017), the respiratory epithelium (Liu *et al.*, 2017), the immune system (Castañeda *et al.*, 2018), and the cardiovascular system (Cao *et al.*, 2016). As skin and keratinocytes form the outermost barrier directly facing harmful PM, the combined effects of $PM_{2.5}$ and UVB on the skin are worth investigating.

Purpurogallin (PG) is a natural phenol (Chang *et al.*, 2014), and phenolic compounds were shown to possess antioxidant effects in cardiovascular diseases, anticancer activity, anti-platelet aggregation effects, and anti-bacterial activity (Faggio *et al.*, 2017). Furthermore, high levels of polyphenols promote collagen synthesis and protect human skin from photo-aging (Kang *et al.*, 2018). PG suppressed delayed vasospasm and suppresses esophageal squamous cell carcinoma growth (Chang *et al.*, 2014, Xie *et al.*, 2019). Additionally, PG reduced inflammation in BV2 microglia cells and osteolytic diseases and showed antioxidant effects (Park *et al.*, 2013; Kim *et al.*, 2018; Li *et al.*, 2022).

As UVB and $PM_{2.5}$ aggravate damage to keratinocytes and as PG may possess cytoprotective effects, this study explored the effects of PG against $PM_{2.5}$- and/or UVB-induced oxidative stress in HaCaT cells, focusing on antioxidant and cytoprotective effects and investigating the underlying mechanisms.

제주대학교 중앙도서관
JEJU NATIONAL UNIVERSITY LIBRARY

RESULTS

Purpurogallin (PG) attenuated ROS generation

According to the MTT assay, PG displayed no cytotoxicity to HaCaT cells through the three tested concentrations (Figure 12A). Cell viability in all treated groups was > 96%, similar to the control. DPPH radical levels were significantly and dose-dependently decreased in PG-treated groups (Figure 12B). The Hydroxyl radical scavenging potential of PG (10 μM) was evaluated using ESR spectrometry. In the positive control ($FeSO_4$ + H_2O_2) system, DMPO/·OH adduct signal was 3366 units and was reduced to 2090 units by PG (Figure 12C). In addition, H_2O_2-induced intracellular ROS were scavenged by PG (Figure 12D). It suggested that PG scavenged intracellular ROS in a concentration-dependent manner in H_2O_2-treated cells, with 10 μM PG scavenging up to 42% ROS, compared to the control.

제주대학교 중앙도서관
JEJU NATIONAL UNIVERSITY LIBRARY

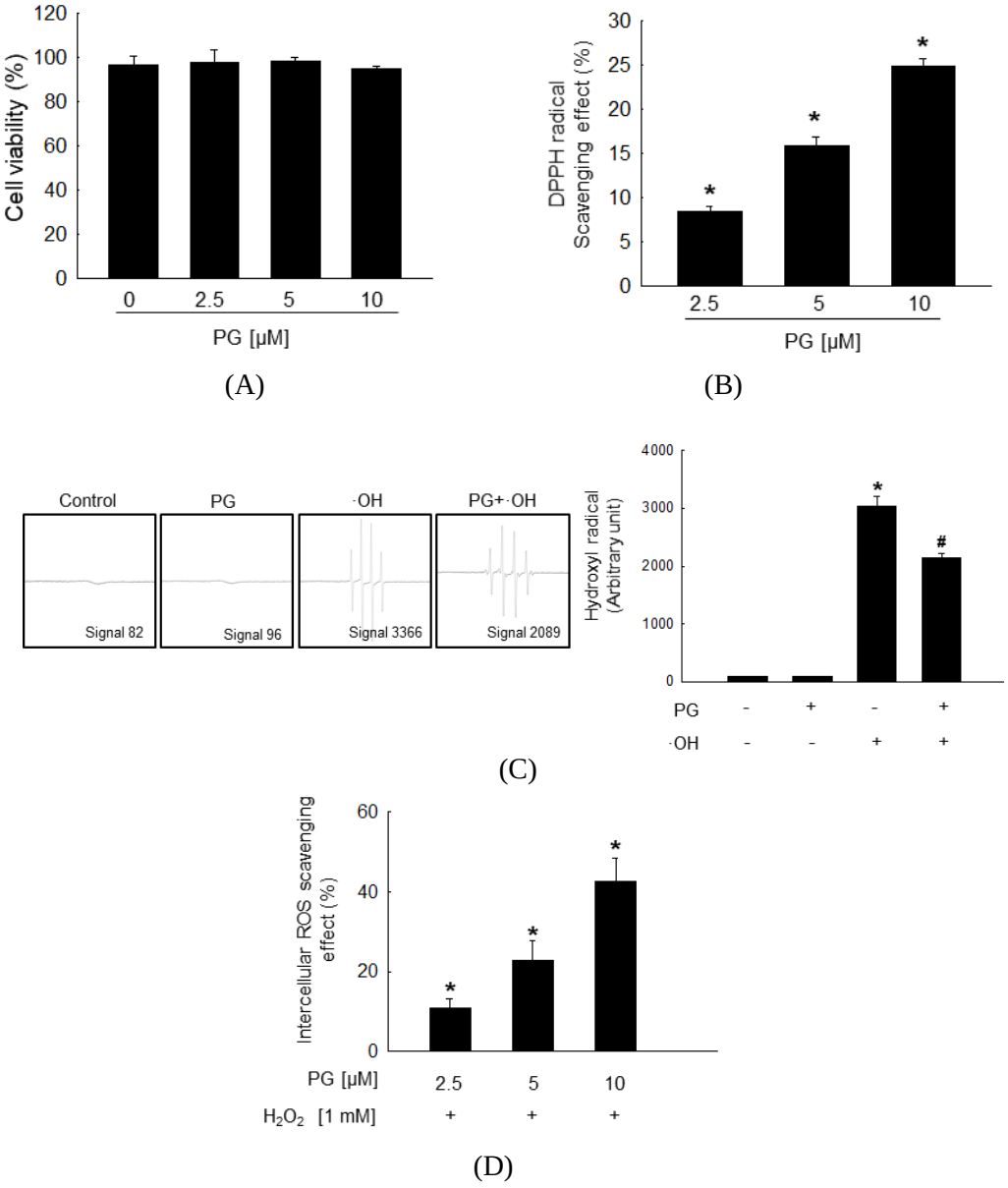

Figure 12. PG reduced the generation of free radicals. (A) The MTT assay was used to determine cell viability after treating HaCaT cells with PG (0, 2.5, 5, and 10 μM) for 24 h. (B) DPPH radical scavenging activity of PG (0, 2.5, 5, and 10 μM). *p < 0.05 vs. positive control. (C) The hydroxyl radical scavenging potential of PG (10 μM) was estimated using the Fenton reaction. *p < 0.05 vs. control, #p < 0.05 vs. ·OH radical, respectively. (D) Intracellular ROS scavenging potential of PG (0, 2.5, 5, 10 μM). ROS generated by H_2O_2 was detected using the H_2DCFDA assay. *p < 0.05 vs. H_2O_2-treated cells.

제주대학교 중앙도서관
JEJU NATIONAL UNIVERSITY LIBRARY

PG protected $PM_{2.5}$-induced cellular macromolecules from oxidative stress

The result showed that 10 μM PG reduced the levels of $PM_{2.5}$-generated intracellular ROS (Figure 13A, 13B). $PM_{2.5}$ generated higher levels of DPPP oxide in cells not treated with PG, compared to PG-pretreated cells (Figure 13C). Additionally, $PM_{2.5}$-exposed cells, which were pretreated with PG, showed lower levels of protein carbonylation than cells not treated with PG (Figure 13D). As for $PM_{2.5}$-induced DNA damage, fluorescence and length of tails were significantly reduced in the PG pretreatment group (from 65 to 22%) (Figure 13E). These results suggested that PG suppressed $PM_{2.5}$-induced ROS generation and protected cellular macromolecules from $PM_{2.5}$-induced damage.

제주대학교 중앙도서관
JEJU NATIONAL UNIVERSITY LIBRARY

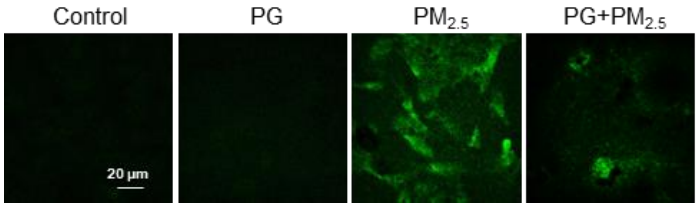

(A)

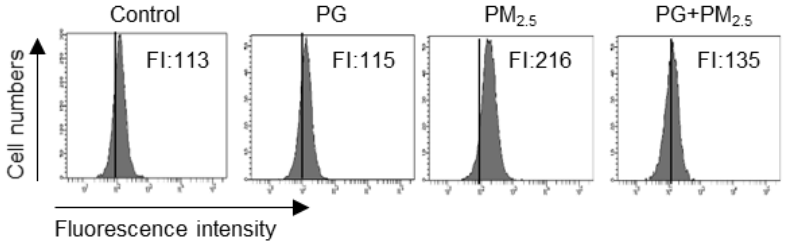

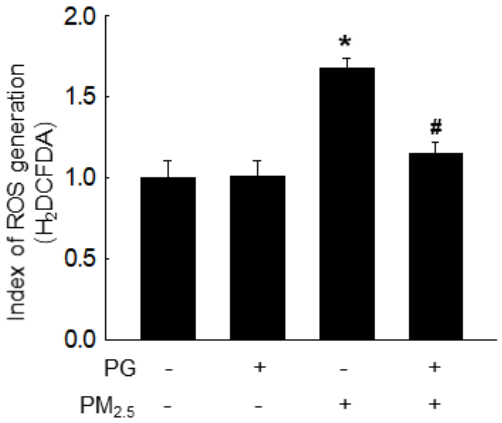

(B)

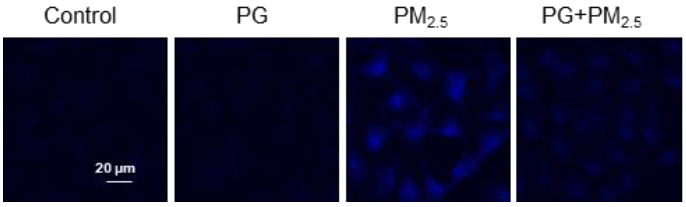

(C)

Figure 13. PG inhibited $PM_{2.5}$-increased ROS generation and macromolecular damage. (A) Confocal microscopy was used for detecting intracellular ROS after H_2DCFDA staining. (B) Intracellular ROS levels were assessed by flow cytometry. (C) Lipid peroxidation was assessed after DPPP staining. *$p < 0.05$ and #$p < 0.05$ vs. control cells and $PM_{2.5}$-exposed cells, respectively.

제주대학교 중앙도서관
JEJU NATIONAL UNIVERSITY LIBRARY

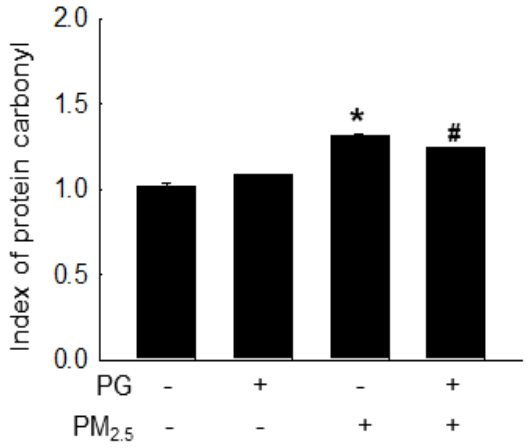

(D)

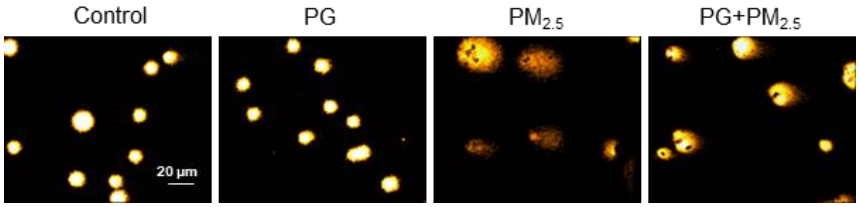

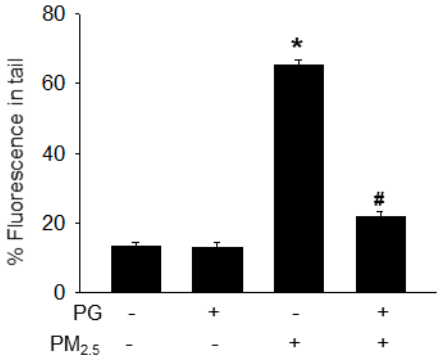

(E)

Figure 13. continued (D) Protein carbonylation assay. (E) Comet assay of the DNA damage. *$p < 0.05$ and #$p < 0.05$ vs. control cells and $PM_{2.5}$-exposed cells, respectively.

제주대학교 중앙도서관
JEJU NATIONAL UNIVERSITY LIBRARY

PG blocked $PM_{2.5}$-induced apoptosis

Using JC-1 staining, normal mitochondrial polarization was observed in $PM_{2.5}$-free cells, whereas $PM_{2.5}$-exposed cells showed indications of mitochondrial depolarization (Figure 14A). The intensity of red and green fluorescence in PG-pretreated cells suggested higher levels of normal mitochondrial polarization and a lower degree of mitochondrial depolarization, compared to mitochondria of the $PM_{2.5}$-exposed group. Flow cytometry confirmed these observations (Figure 14B). Additionally, Hoechst 33342 staining of apoptotic bodies indicated that the $PM_{2.5}$-exposed cell group presented the highest number of apoptotic cells, whereas cells pretreated with PG avoided apoptosis to a certain degree (Figure 14C).

제주대학교 중앙도서관
JEJU NATIONAL UNIVERSITY LIBRARY

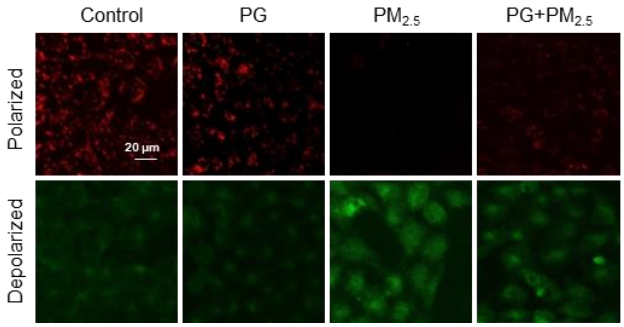

(A)

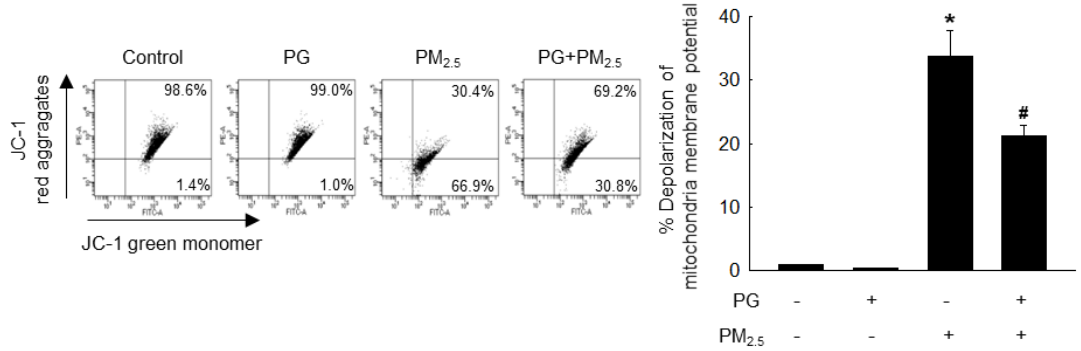

(B)

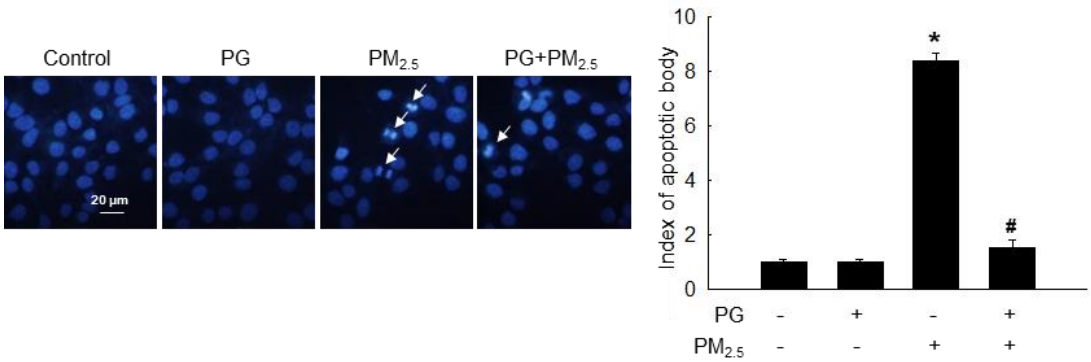

(C)

Figure 14. $PM_{2.5}$ caused apoptosis via mitochondrial dysfunction. Cells were stained with JC-1 to detect the mitochondrial membrane potential (ΔΨm) by (A) confocal microscopy and (B) flow cytometry. (C) Apoptotic bodies (arrows) stained with Hoechst 33342. *$p < 0.05$ and #$p < 0.05$ vs. control cells and $PM_{2.5}$-exposed cells, respectively.

제주대학교 중앙도서관
JEJU NATIONAL UNIVERSITY LIBRARY

PG protected cells against $PM_{2.5}$- and UVB-induced apoptosis

To confirm that $PM_{2.5}$ aggravates UVB-induced damage to keratinocytes, intracellular ROS levels were analyzed. Intracellular ROS levels were increased by $PM_{2.5}$ and/or UVB, whereas PG (10 μM) decreased ROS levels induced by $PM_{2.5}$ and/or UVB (Figure 15A). Lipid peroxidation was investigated by DPPP staining. $PM_{2.5}$ combined with UVB induced a high degree of lipid peroxidation, and outranking UVB irradiation alone, whereas lipid peroxidation induced by $PM_{2.5}$ and/or UVB in PG-treated cells was considerably lower (Figure 15B), indicating that PG ameliorated lipid peroxidation induced by these factors. $PM_{2.5}$- and/or UVB-induced DNA damage was analyzed using the comet assay (Figure 15C). Compared to UVB, $PM_{2.5}$ prolonged comet tails, whereas PG shortened comet tails in cells treated with $PM_{2.5}$ and/or UVB. Additionally, Hoechst 33342 staining indicated that $PM_{2.5}$ promoted UVB-induced apoptosis, whereas pretreatment with PG partially protected cells from $PM_{2.5}$- and/or UVB-induced apoptosis (Figure 15D). Taken together, these results suggest that PG possesses cytoprotective effects against $PM_{2.5}$- and/or UVB-induced oxidative damage and apoptosis.

제주대학교 중앙도서관
JEJU NATIONAL UNIVERSITY LIBRARY

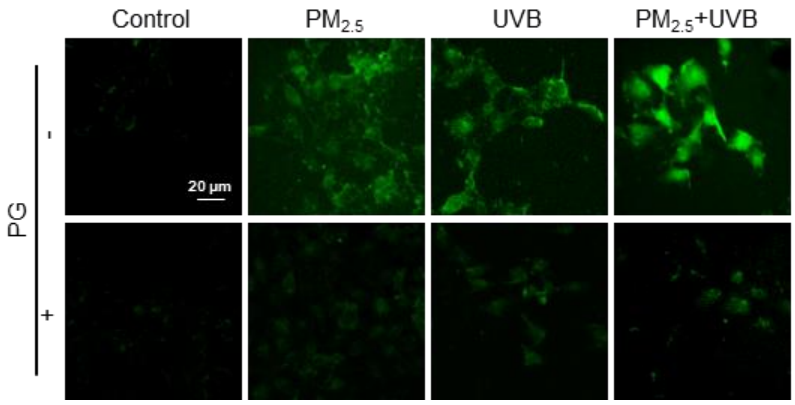

(A)

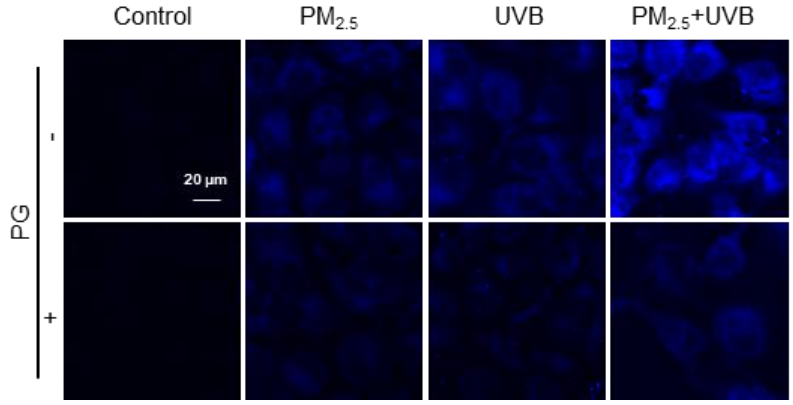

(B)

Figure 15. UVB enhanced $PM_{2.5}$-induced apoptosis, which was decreased by PG. (A) Cells were stained by H_2DCFDA for detecting intracellular ROS induced by $PM_{2.5}$ and/or UVB. (B) Lipid peroxidation induced by $PM_{2.5}$ and/or UVB was detected after DPPP staining.

제주대학교 중앙도서관
JEJU NATIONAL UNIVERSITY LIBRARY

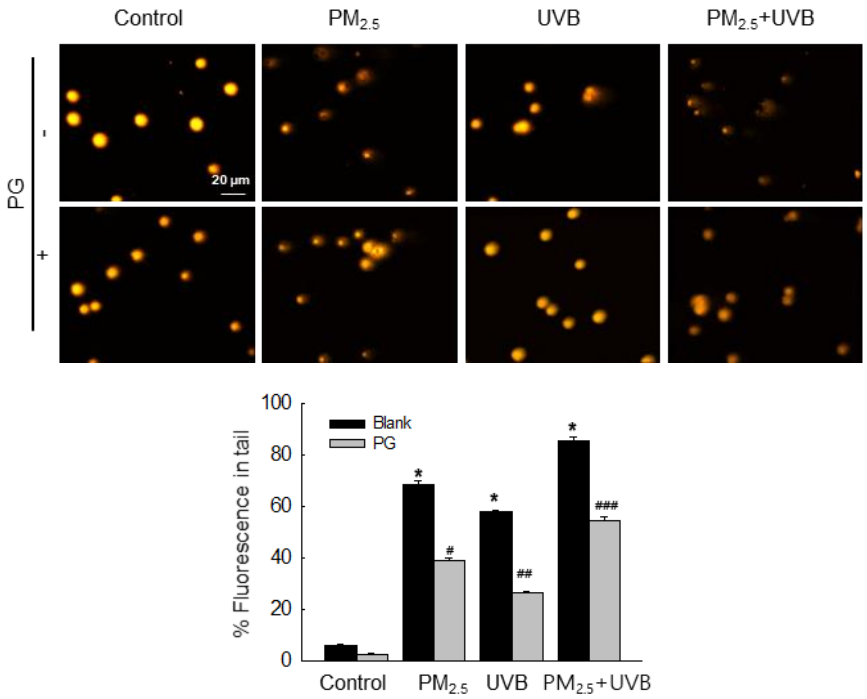

(C)

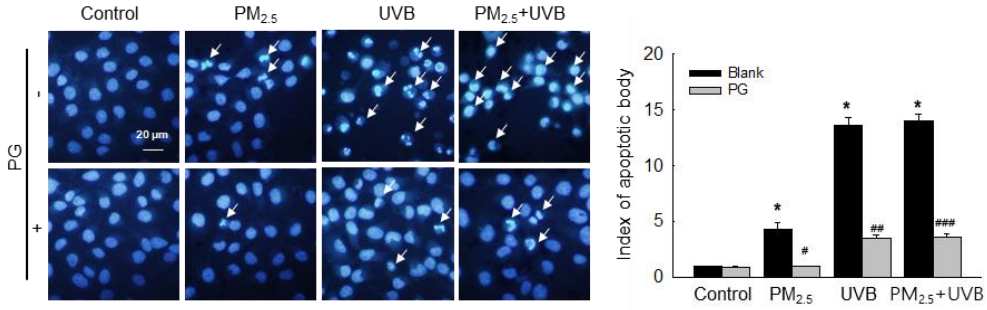

(D)

Figure 15. continued (C) Comet assay cellular tail lengths induced by $PM_{2.5}$ and/or UVB. (D) Fluorescence microscopy was used to detect Hoechst 33342-stained apoptotic bodies (arrows) induced by $PM_{2.5}$ and/or UVB. *$p < 0.05$, #$p < 0.05$ ##$p < 0.05$ and ###$p < 0.05$ vs. control cells, UVB-irradiated cells, $PM_{2.5}$-treated cells, and $PM_{2.5}$-treated and UVB-irradiated cells, respectively.

제주대학교 중앙도서관
JEJU NATIONAL UNIVERSITY LIBRARY

DISCUSSION

$PM_{2.5}$ (with a particle diameter of < 2.5 μm) can reach the lungs and stimulate ROS production in the skin, increasing oxidative stress (Piao *et al.*, 2018). High ROS levels disrupt the normal function of the endoplasmic reticulum, mitochondria, and lysosomes, leading to apoptosis. Additionally, the skin is the largest human organ and it is susceptible to irritation and sunburns through UV exposure. Moreover, epidemiological studies have indicated that UVB suppresses immune reactions, promotes ROS generation, and damages cell membrane proteins and lipids (Boakye *et al.*, 2016). UVB-induced ROS production is also reported to be a major cause of skin cancer, as it results in the formation of 8-hydroxy-2′-deoxyguanine (Agar *et al.*, 2004).

This study evaluated the cytoprotective effects of PG on oxidative stress and apoptosis. Our results show that $PM_{2.5}$ increased intracellular ROS production and caused macromolecule damage and apoptosis. In human HaCaT cells, $PM_{2.5}$ exposure resulted in the dysfunction of mitochondria and a high apoptosis index. Notably, $PM_{2.5}$ aggravated UVB-induced skin damage (Figure 15), increasing oxidative stress, damaging DNA, exacerbating lipid peroxidation, and increasing the number of apoptotic bodies. PG pretreatment reduced cellular ROS levels and consequently resulted in fewer apoptotic bodies.

Taken together, these results show that $PM_{2.5}$ and UVB irradiation contributed to apoptosis. These results suggest that PG could be potentially used in protecting the skin from UVB irradiation and $PM_{2.5}$.

제주대학교 중앙도서관
JEJU NATIONAL UNIVERSITY LIBRARY

CONCLUSION

In conclusion, the tested phenolic compounds ameliorated $PM_{2.5}$-induced skin keratinocyte damage by inhibiting ROS generation and macromolecular oxidation. In addition, both DPHC and eckol could sustain ER and mitochondrial homeostasis, and reduce apoptosis by the MAPK signaling pathway. In terms of PG, it could protect cells from both $PM_{2.5}$ and UVB insults by inhibiting oxidative stress and DNA damage.

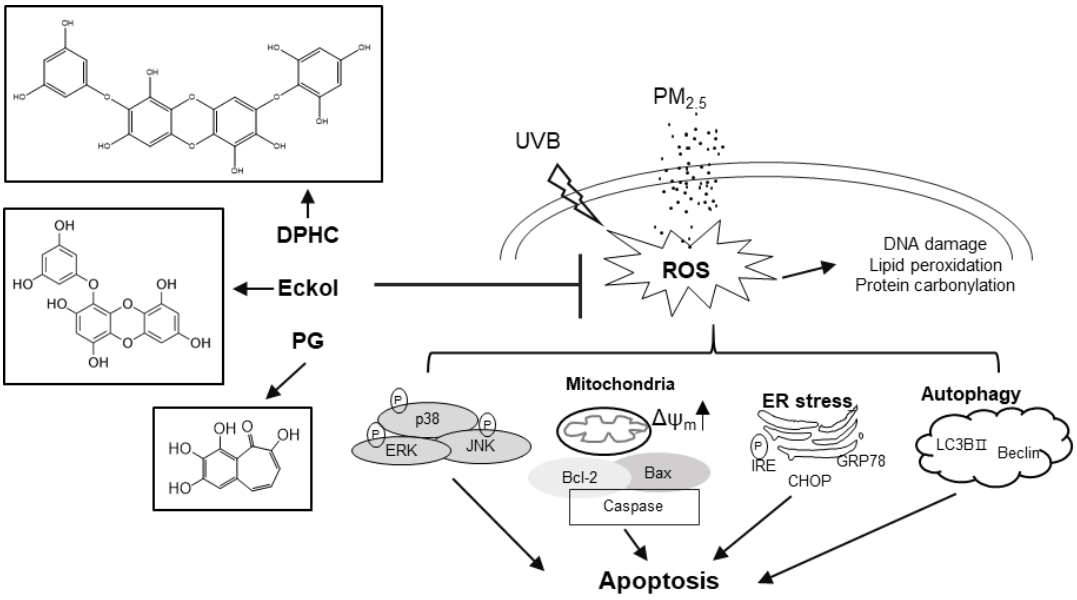

Figure 16. Mechanism of protective effects of phenolic compounds (DPHC, eckol, and PG) on $PM_{2.5}$-induced skin damage.

제주대학교 중앙도서관
JEJU NATIONAL UNIVERSITY LIBRARY

MATERIALS AND METHODS

Samples and $PM_{2.5}$ and UVB application

DPHC and eckol were provided by Professor Nam Ho Lee of Jeju National University (Jeju, Republic of Korea). PG and diesel $PM_{2.5}$ of SRM 1650b were purchased from the company of Sigma-Aldrich (St. Louis, MO, USA). All samples (DPHC, eckol, and PG) of concentration at 100 mM and $PM_{2.5}$ at 25 mg/mL were dissolved into dimethyl sulfoxide as stock solutions. The UVB energy spectrum (280 - 320 nm) was supplied by CL-1000M UV Crosslinker (UVP, Upland, CA, USA). UVB irradiation dose was 30 mJ/cm^2.

Experiments in vitro

The HaCaT cell line of human keratinocytes was provided by Cell Lines Service (Heidelberg, Germany), which were seeded into Dulbecco's modified Eagle's medium (Life Technologies Co., Grand Island, NY, USA) with a humidified environment under an incubator providing 37°C and 5% CO_2. The 10% heat-inactivated fetal calf serum and 1% antibiotic-antimycotic both obtained from Life Technologies Co. were added into the culture medium.

Experiments in vivo

In vivo experiments were performed using HR-1 hairless male mouse (OrientBio, Kyungki-do, Republic of Korea) in accordance with Jeju National University's guidelines for the care and use of laboratory animals (Jeju, Republic of Korea; permit number: 2017-0026). The 16 mice for experiments were randomly assigned to four groups (n=4) as groups of control, $PM_{2.5}$-treated, DPHC low dose (200 μM + $PM_{2.5}$), and DPHC high dose (2 mM + $PM_{2.5}$). The nonwoven polyethylene pads with $PM_{2.5}$ (100 μg/mL) in a 1 cm^2 area were applied on the mouse dorsal skin for constant 7 days, and the treated skins by dissection were used for biochemical and histological analyses.

제주대학교 중앙도서관
JEJU NATIONAL UNIVERSITY LIBRARY

Cell viability

Cells at the density of 0.8×10^5 cells/mL were plated into a 24-well plate. Then cell viabilities according to the formation of formazan crystals in each well with MTT solution (2 mg/mL) were detected. The absorbance of each well was measured by a scanning multi-well spectrophotometer at 540 nm.

DPPH radical detection

The antiradical activity was detected with DPPH (Sigma-Aldrich), a free radical agent. The samples of DPHC (final concentration of 0, 2.5, 5, 10, 20, or 40 μM) and PG (final concentration of 0, 2.5, 5, or, 10 μM) were mixed with 0.1 mM DPPH, which were mildly shaken in dark for 3 h. The absorbances of residual DPPH solutions were measured with a spectrophotometer at 520 nm.

Scavenging ability of ROS

Cells were treated with samples of DPHC, eckol, or PG for 30 min, and stimulated by $PM_{2.5}$ for another 30 min, which was then dyed with H_2DCFDA (Molecular Probes, Eugene, OR, USA) or DHR123 (Molecular Probes) for 30 min. The FV1200 laser scanning confocal microscope (Olympus, Tokyo, Japan) and a FACS Calibur flow cytometer (Becton Dickinson, Mountain View, CA, USA) were used to visualize and analyze the value of intracellular ROS, respectively.

Lipid peroxidation assay

Cells were treated with samples of DPHC, eckol, or PG for 30 min, and cocultured with $PM_{2.5}$ for another 24 h, which was then dyed with DPPP (Molecular Probes). The fluorescent images of lipid peroxidation were captured under a confocal microscope.

8-Oxoguanine observation

Cells were treated with samples of DPHC or eckol for 30 min and exposed to $PM_{2.5}$ for another 24 h, which was then stained with avidin-TRITC conjugate (Sigma-Aldrich). A confocal microscope was for image observation.

제주대학교 중앙도서관
JEJU NATIONAL UNIVERSITY LIBRARY

Single-cell gel electrophoresis (comet assay)

Comet assay was used for the detection of single-strand or double-strand DNA breaks by the method of single-cell gel electrophoresis. Individual cells were applied on slides and embedded in a thin agarose gel. After unwinding and electrophoresis, the dried slides were stained with ethidium bromide for observation of the comet head and tail representing intact and stands of DNA, respectively. The image analysis software (Kinetic Imaging, Komet 5.5, UK) was used for recording data on the tail length of 50 cells per slide.

Western blotting

Cell lysates were separated using sodium dodecyl sulfate-polyacrylamide gel electrophoresis (SDS-PAGE), and the separated proteins were transferred onto membranes. Then, the membranes were incubated with primary antibodies and secondary antibodies, separately. Finally, the Amersham enhanced chemiluminescence plus western blotting detection system (GE Healthcare Life Sciences, Buckinghamshire, UK) was used to detect the protein bands. The primary antibodies were as followed: phospho-H2A.X, phospho-IRE1α, CHOP, Beclin-1, LC3B, caspase-9, caspase-3, phospho-ERK, phospho-p38, p38, phospho-JNK, and JNK (Cell Signaling Technology, Beverly, MA, USA); Bcl-2, Bax, and ERK2 (Santa Cruz Biotechnology, Santa Cruz, CA, USA); actin (Sigma-Aldrich). The secondary antibody was obtained from Pierce (Rockford, IL, USA).

8-Isoprostane assay

Following the manufacturer's instructions, the Oxiselect^{TM} 8-iso-Prostaglandin F2α ELISA kit (Cell Biolabs, San Diego, CA, USA) of the enzyme immunoassay was used to measure the amounts of 8-isoprostane in the mice's skin tissue.

Protein carbonylation

The protein oxidation level of harvested cells and lysates of mouse skin was detected with Oxiselect^{TM} protein carbonyl enzyme-linked immunosorbent assay (ELISA) kit (Cell Biolabs, San Diego, CA, USA) according to the manufacturer’s instructions.

제주대학교 중앙도서관
JEJU NATIONAL UNIVERSITY LIBRARY

Ca^{2+} level detection

Harvested cells were applied to the confocal microscope and flow cytometer for detecting intracellular and mitochondrial Ca^{2+} levels with Fluo-4 AM (Molecular Probes) and Rhod-2 AM (Molecular Probes), respectively.

Acridine orange morphology assay

Cells were treated with samples and/or exposed to $PM_{2.5}$ for 24 h. The images of harvested cells with acridine orange (Invitrogen) were collected with a fluorescence microscope.

Membrane potential analysis

The collected cells' membrane potential was analyzed using the confocal microscope and flow cytometer after staining probe JC-1 (Invitrogen, Carlsbad, CA, USA).

Sub-G_1 DNA content assay

Collected cells were fixed with 70% ethanol and stained with PI dye (50 mg/mL) solution containing RNase A. Then DNA contents in cells were analyzed by a flow cytometer and the sub-G_1 population in each group was obtained.

Apoptotic assay (Hoechst 33342)

$PM_{2.5}$ were applied to the cells after treatment with samples and/or inhibitors, and 24 h later, the DNA in keratinocytes was dyed with Hoechst 33342 (Sigma-Aldrich), which was captured by a fluorescence microscope with a CoolSNAP-Pro color digital camera (Media Cybernetics, Rockville, MD, USA).

Hydroxyl radical scavenging

The Fenton reaction ($FeSO_4 + H_2O_2$) system was applied to assess the scavenging ability of hydroxyl radicals under an ESR spectrometer by detecting DMPO/·OH adduct. The ESR spectrometer parameters were as follows: central magnetic field 336.8 mT, power 1.00 mW, frequency 9.4380 GHz, modulation width 0.2 mT, amplitude 600, sweep width 10 mT, sweep time 0.5 min, gain 200, time constant 0.03 s, and temperature 25°C.

제주대학교 중앙도서관
JEJU NATIONAL UNIVERSITY LIBRARY

Statistical analysis

The SigmaStat 3.5 (Systat Software Inc., San Jose, CA, USA) was used to examine the statistical significance among various groups. A p-value < 0.05 was regarded as statistically significant for all of the data.

제주대학교 중앙도서관
JEJU NATIONAL UNIVERSITY LIBRARY

REFERENCES

Ain NU; Qamar SUR. Particulate matter-induced cardiovascular dysfunction: A mechanistic insight. Cardiovasc Toxicol 2021;21:505-516.

Agar NS; Halliday GM; Barnetson RS; Ananthaswamy HN; Wheeler M; Jones AM. The basal layer in human squamous tumors harbors more UVA than UVB fingerprint mutations: A role for UVA in human skin carcinogenesis. Proc Natl Acad Sci USA 2004;101:4954-4959.

Almeida SM; Manousakas M; Diapouli E; Kertesz Z; Samek L; Hristova E; Šega K; Alvarez RP; Belis CA; Eleftheriadis K. IAEA European region study GROUP Ambient particulate matter source apportionment using receptor modelling in european and central asia urban areas. Environ Pollut 2020;266:115199.

Asweto CO; Wu J; Alzain MA; Hu H; Andrea S; Feng L; Yang X; Duan J; Sun Z. Cellular pathways involved in silica nanoparticles induced apoptosis: A systematic review of in vitro studies. Environ Toxicol Pharmacol 2017;56:191-197.

Bae YJ; Park KY; Han HS; Kim YS; Hong JY; Han TY; Seo SJ. Effects of particulate matter in a mouse model of oxazolone-induced atopic dermatitis. Ann Dermatol 2020;32:496-507.

Boakye CHA; Patel K; Doddapaneni R; Bagde A; Behl G; Chowdhury N; Safe S; Singh M. Ultra-flexible nanocarriers for enhanced topical delivery of a highly lipophilic antioxidative molecule for skin cancer chemoprevention. Colloids Surf B 2016;143:156-167.

Bosch R; Philips N; Suárez-Pérez JA; Juarranz A; Devmurari A; Chalensouk-Khaosaat J; González S. Mechanisms of photoaging and cutaneous photocarcinogenesis, and photoprotective strategies with phytochemicals. Antioxidants 2015; 4:248-268.

제주대학교 중앙도서관
JEJU NATIONAL UNIVERSITY LIBRARY

Cao J; Qin G; Shi R; Bai F; Yang G; Zhang M; Lv J. Overproduction of reactive oxygen species and activation of MAPKs are involved in apoptosis induced by PM2.5 in rat cardiac H9c2 cells. J Appl Toxicol 2016;36:609-617.

Castañeda AR; Pinkerton KE; Bein KJ; Magaña-Méndez A; Yang HT; Ashwood P; Vogel CFA. Ambient particulate matter activates the aryl hydrocarbon receptor in dendritic cells and enhances Th17 polarization. Toxicol Lett 2018;292:85-96.

Chang CZ; Lin CL; Wu SC; Kwan AL. Purpurogallin, a natural phenol, attenuates high-mobility group box 1 in subarachnoid hemorrhage induced vasospasm in a rat model. Int J Vasc Med 2014;2014:254270.

Chang MY; Byon SH; Shin HC; Han SE; Kim JY; Byun JY; Lee JD; Park MK. Protective effects of the seaweed phlorotannin polyphenolic compound dieckol on gentamicin-induced damage in auditory hair cells. Int J Pediatr Otorhinolaryngol 2016;83:31-36.

Chaudhary AK; Yadav N; Bhat TA; O'Malley J; Kumar S; Chandra D. A potential role of X-linked inhibitor of apoptosis protein in mitochondrial membrane permeabilization and its implication in cancer therapy. Drug Discov Today 2016;21:38-47.

Cho SH; Kim HS; Lee W; Han EJ; Kim SY; Fernando IPS; Ahn G; Kim KN. Eckol from Ecklonia cava ameliorates TNF-α/IFN-γ-induced inflammatory responses via regulating MAPKs and NF-κB signaling pathway in HaCaT cells. Int Immunopharmacol 2020;82:106146.

Chuang KC; Chang CR; Chang SH; Huang SW; Chuang SM; Li ZY; Wang ST; Kao JK; Chen YJ; Shieh JJ. Imiquimod-induced ROS production disrupts the balance of mitochondrial dynamics and increases mitophagy in skin cancer cells. J Dermatol Sci 2020;98:152-162.

Czabotar PE; Lessene G; Strasser A; Adams JM. Control of apoptosis by the BCL-2 protein family: implications for physiology and therapy. Nat Rev Mol Cell Biol 2014;15:49-63.

제주대학교 중앙도서관
JEJU NATIONAL UNIVERSITY LIBRARY

Diao P; He H; Tang J; Xiong L; Li L. Natural compounds protect the skin from airborne particulate matter by attenuating oxidative stress. Biomed Pharmacother 2021;138:111534.

Dijkhoff IM; Drasler B; Karakocak BB; Petri-Fink A; Valacchi G; Eeman M; Rothen-Rutishauser B. Impact of airborne particulate matter on skin: a systematic review from epidemiology to in vitro studies. Part Fibre Toxicol 2020;17:35

Faggio C; Sureda A; Morabito S; Sanches-Silva A; Mocan A; Nabavi SF; Nabavi SM Flavonoids and platelet aggregation: A brief review. Eur J Pharmacol 2017;807:91-101.

Gheda S; Naby MA; Mohamed T; Pereira L; Khamis A. Antidiabetic and antioxidant activity of phlorotannins extracted from the brown seaweed Cystoseira compressa in streptozotocin-induced diabetic rats. Environ Sci Pollut Res Int 2021;28:22886-22901.

Ghosh D; LeVault KR; Barnett AJ; Brewer GJ. A reversible early oxidized redox state that precedes macromolecular ROS damage in aging nontransgenic and 3xTg-AD mouse neurons. J Neurosci 2012;32:5821-5832.

Grether-Beck S; Felsner I; Brenden H; Marini A; Jaenicke T; Aue N; Welss T; Uthe I; Krutmann J. Air pollution-induced tanning of human skin. Br J Dermatol 2021;185:1026-1034.

Gu Y; Han J; Jiang C; Zhang Y. Biomarkers, oxidative stress and autophagy in skin aging. Ageing Res Rev 2020;59:101036

Guarnieri M; Balmes JR. Outdoor air pollution and asthma. Lancet 2014;383:1581-1592.

Gupta R; Ambasta RK; Kumar P. Autophagy and apoptosis cascade: Which is more prominent in neuronal death? Cell Mol Life Sci 2021;78:8001-8047.

He M; Ichinose T; Yoshida S; Shiba F; Arashidani K; Takano H; Sun G; Shibamoto T. Differences in allergic inflammatory responses in murine lungs: Comparison of PM2.5

제주대학교 중앙도서관
JEJU NATIONAL UNIVERSITY LIBRARY

and coarse PM collected during the hazy events in a Chinese city. Inhal Toxicol 2016;28:706-718.

Heo SJ; Kim JP; Jung WK; Lee NH; Kang HS; Jun EM; Park SH; Kang SM; Lee YJ; Park PJ; *et al.* Identification of chemical structure and free radical scavenging activity of diphlorethohydroxycarmalol isolated from a brown alga, ishige okamurae. J Microbiol Biotechnol 2008;18:676-681.

Hu R; Xie XY; Xu SK; Wang YN; Jiang M; Wen LR; Lai W; Guan L. PM2.5 exposure elicits oxidative stress responses and mitochondrial apoptosis pathway activation in HaCaT keratinocytes. Chin Med J 2017;130:2205-2214.

Hu M; Yang X; Chang X. Bioactive phenolic components and potential health effects of chestnut shell: A review. J Food Biochem 2021;45:e13696.

Huang PH; Tseng CH; Lin CY; Lee CW; Yen FL. Preparation, characterizations and anti-pollutant activity of 7,3',4'-trihydroxyisoflavone nanoparticles in particulate matter-induced HaCaT keratinocytes. Int J Nanomedicine 2018;13:3279-3293.

Hyun YJ; Piao MJ; Kang KA; Zhen AX; Fernando PDSM; Kang HK; Ahn YS; Hyun JW. Effect of fermented fish oil on fine particulate matter-induced skin aging. Mar Drugs 2019;17:61.

Jeanson A; Boyer A; Greillier L; Tomasini P; Barlesi F. Therapeutic potential of trametinib to inhibit the mutagenesis by inactivating the protein kinase pathway in non-small cell lung cancer. Expert Rev Anticancer Ther 2019;19:11-17.

Jin Y; Zhu M; Guo Y; Foreman D; Feng F; Duan G; Wu W; Zhang W. Fine particulate matter PM2.5 enhances FcεRI-mediated signaling and mast cell function. Cell Signal 2019;57:102-109.

제주대학교 중앙도서관
JEJU NATIONAL UNIVERSITY LIBRARY

Joe MJ; Kim SN; Choi HY; Shin WS; Park GM; Kang DW; Kim YK. The inhibitory effects of eckol and dieckol from Ecklonia stolonifera on the expression of matrix metalloproteinase-1 in human dermal fibroblasts. Biol Pharm Bull 2006;29:1735-1739.

Jun MS; Kwack MH; Kim MK; Kim JC; Sung YK. Particulate matters induce apoptosis in human hair follicular keratinocytes. Ann Dermatol 2020;32:388-394.

Kang CH; Rhie SJ; Kim YC. Antioxidant and skin anti-aging effects of marigold methanol extract. Toxicol Res 2018;34:31-39.

Kang NJ; Han SC; Kan GJ; Koo DH; Koh YS; Hyun JW; Lee NH; Ko MH; Kang HK; Yoo ES. Diphlorethohydroxycarmalol inhibits interleukin-6 production by regulating NF-kB, stat5 and socs1 in lipopolysaccharide-stimulated raw 2647 cells. Mar Drugs 2015a;13:2141-2157.

Kang NJ; Koo DH; Kang GJ; Han SC; Lee BW; Koh YS; Hyun JW; Lee NH; Ko MH; Kang HK; *et al.* Dieckol, a component of ecklonia cava, suppresses the production of MDC/CCL22 via down-regulating STAT1 pathway in interferon-γ stimulated HaCaT human keratinocytes. Biomol Ther 2015b;23:238-244.

Kang YJ; Tan HY; Lee CY; Cho H. An air particulate pollutant induces neuroinflammation and neurodegeneration in human brain models. Adv Sci Weinh 2021;8:e2101251.

Kiang JG; Olabisi AO. Radiation: A poly-traumatic hit leading to multi-organ injury. Cell Biosci 2019;9:25.

Kim AD; Kang KA; Piao MJ; Kim KC; Zheng J; Yao CW; Cha JW; Hyun CL; Kang HK; Lee NH; *et al.* Cytoprotective effect of eckol against oxidative stress-induced mitochondrial dysfunction: Involvement of the FoxO3a/AMPK pathway. J Cell Biochem 2014;115:1403-1411.

Kim JH; Lee S; Park S; Park JS; Kim YH; Yang SY. Slow-Binding Inhibition of Tyrosinase by Ecklonia cava Phlorotannins. Mar Drugs 2019;17:359.

제주대학교 중앙도서관
JEJU NATIONAL UNIVERSITY LIBRARY

Kim K; Kim TH; Ihn HJ; Kim JE; Choi JY; Shin HI; Park EK. Inhibitory effect of purpurogallin on osteoclast differentiation in vitro through the downregulation of c-Fos and NFATc1. Int J Mol Sci 2018;19:E601.

Kim KC; Kang KA; Zhang R; Piao MJ; Kim GY; Kang MY; Lee SJ; Lee NH; Surh YJ; Hyun JW. Up-regulation of Nrf2-mediated heme oxygenase-1 expression by eckol, a phlorotannin compound, through activation of Erk and PI3K/Akt. Int J Biochem Cell Biol 2010;42:297-305.

Kim KE; Cho D; Park HJ. Air pollution and skin diseases: Adverse effects of airborne particulate matter on various skin diseases. Life Sci 2016;152:126-134.

Kim KH; Jahan SA; Kabir E. A review on human health perspective of air pollution with respect to allergies and asthma. Environ Int 2013;59:41-52.

Kim KH; Kabir E; Kabir S. A review on the human health impact of airborne particulate matter. Environ Int 2015;74:136-143.

Kim YM; Kim J; Ha SC; Ahn K. Effects of exposure to indoor fine particulate matter on atopic dermatitis in children. Int J Environ Res Public Health 2021;18:11509.

Kong CS; Kim JA; Ahn BN; Kim SK. Potential effect of phloroglucinol derivatives from Ecklonia cava on matrix metalloproteinase expression and the inflammatory profile in lipopolysaccharide-stimulated human THP-1 macrophages. Fish Sci 2011;77:867-873.

Krutmann J; Liu W; Li L; Pan X; Crawford M; Sore G; Seite S. Pollution and skin: From epidemiological and mechanistic studies to clinical implications. J Dermatol Sci 2014;76:163-168.

Li D; Li Y; Li G; Zhang Y; Li J; Chen H. Fluorescent reconstitution on deposition of PM2.5 in lung and extrapulmonary organs. Proc Natl Acad Sci USA 2019;116:2488-2493.

제주대학교 중앙도서관
JEJU NATIONAL UNIVERSITY LIBRARY

Li Q; Kang Z; Jiang S; Zhao J; Yan S; Xu F; Xu J. Effects of ambient fine particles PM2.5 on human HaCaT cells. Int J Environ Res Public Health 2017;14:E72.

Li X; Cheng Z; Chen X; Yang D; Li H; Deng Y. Purpurogallin improves neurological functions of cerebral ischemia and reperfusion mice by inhibiting endoplasmic reticulum stress and neuroinflammation. Int Immunopharmacol 2022;111:109057.

Lim JU; Yoon HK. Narrative review: Association between lung cancer development and ambient particulate matter in never-smokers. J Thorac Dis 2022;14:553-563.

Liu Q; Xu C; Ji GX; Liu H; Shao W; Zhang C; Gu A; Zhao P. Effect of exposure to ambient PM2.5 pollution on the risk of respiratory tract diseases: A meta-analysis of cohort studies. J Biomed Res 2017;31:130-142.

Magnano GC; Marussi G; Pavoni E; Adami G; Larese Filon F; Crosera M. Percutaneous metals absorption following exposure to road dust powder. Environ Pollut 2022;292:118353.

Magnani ND; Muresan XM; Belmonte G; Cervellati F; Sticozzi C; Pecorelli A; Miracco C; Marchini T; Evelson P; Valacchi G. Skin damage mechanisms related to airborne particulate matter exposure. Toxicol Sci 2016;149:227-236.

Marrot L. Pollution and sun exposure: A deleterious synergy mechanisms and opportunities for skin protection. Curr Med Chem 2018;25:5469-5486.

Mayer AM; Hamann MT. Marine pharmacology in 2001-2002: Marine compounds with anthelmintic, antibacterial, anticoagulant, antidiabetic, antifungal, anti-inflammatory, antimalarial, antiplatelet, antiprotozoal, antituberculosis, and antiviral activities; affecting the cardiovascular, immune and nervous systems and other miscellaneous mechanisms of action. Comp Biochem Physiol C Toxicol Pharmacol 2005;140:265-286.

Mei Y; Thompson MD; Cohen RA; Tong X. Endoplasmic reticulum stress and related pathological processes. J Pharmacol Biomed Anal 2013;1:1000107.

제주대학교 중앙도서관
JEJU NATIONAL UNIVERSITY LIBRARY

Misra N; Marrot L. In vitro methods to simulate pollution and photo-pollution exposure in human skin epidermis. Methods Mol Biol 2020;2150:227-241.

Moldoveanu T; Follis AV; Kriwacki RW; Green DR. Many players in BCL-2 family affairs. Trends Biochem Sci 2014;39:101-111.

Monteiro P; Lomartire S; Cotas J; Marques JC; Pereira L; Gonçalves AMM. Call the eckols: Present and future potential cancer therapies. Mar Drugs 2022;20:387.

Morita A. Tobacco smoke causes premature skin aging. J Dermatol Sci 2007;48:169-175.

Nishitoh H. CHOP is a multifunctional transcription factor in the ER stress response. J Biochem 2012;151:217-219.

Ngoc LTN; Park D; Lee Y; Lee YC. Systematic review and meta-analysis of human skin diseases due to particulate matter. Int J Environ Res Public Health 2017;14:1458.

Pan H; Wang Y; Na K; Wang Y; Wang L; Li Z; Guo C; Guo D; Wang X. Autophagic flux disruption contributes to Ganoderma lucidum polysaccharide-induced apoptosis in human colorectal cancer cells via MAPK/ERK activation. Cell Death Dis 2019;10:456.

Pan TL; Wang PW; Aljuffali IA; Huang CT; Lee CW; Fang JY. The impact of urban particulate pollution on skin barrier function and the subsequent drug absorption. J Dermatol Sci 2015;78:51-60.

Pauly M; Angebault-Prouteau C; Dridi H; Notarnicola C; Scheuermann V; Lacampagne A; Matecki S; Fauconnier J. ER stress disturbs SR/ER-mitochondria Ca2+ transfer: Implications in Duchenne muscular dystrophy. Biochim. Biophys Acta Mol Basis Dis 2017;1863:2229-2239.

Park E; Ahn GN; Lee NH; Kim JM; Yun JS; Hyun JW; Jeon YJ; Wie MB; Lee YJ; Park JW; *et al.* Radioprotective properties of eckol against ionizing radiation in mice. FEBS Lett 2008;582:925-930.

제주대학교 중앙도서관
JEJU NATIONAL UNIVERSITY LIBRARY

Park HY; Kim TH; Kim CG; Kim GY; Kim CM; Kim ND; Kim BW; Hwang HJ; Choi YH. Purpurogallin exerts anti-inflammatory effects in lipopolysaccharide-stimulated BV2 microglial cells through the inactivation of the NF-κB and MAPK signaling pathways. Int J Mol Med 2013;32:1171-1178.

Peng F; Tsuji G; Zhang JZ; Chen Z; Furue M. Potential role of PM2.5 in melanogenesis. Environ Int 2019;132:105063.

Piao MJ; Ahn MJ; Kang KA; Ryu YS; Hyun Y; Shilnikova K; Zhen AX; Jeong JW; Choi YH; Kang HK; *et al.* Particulate matter 25 damages skin cells by inducing oxidative stress, subcellular organelle dysfunction, and apoptosis. Arch Toxicol 2018;92:2077-2091.

Piao MJ; Hewage SR; Han X; Kang KA; Kang HK; Lee NH; Hyun JW. Protective effect of diphlorethohydroxycarmalol against ultraviolet B radiation-induced DNA damage by inducing the nucleotide excision repair system in HaCaT human keratinocytes. Mar Drugs 2015b;13:5629-5641.

Piao MJ; Kang KA; Kim KC; Chae S; Kim GO; Shin T; Kim HS; Hyun JW. Diphlorethohydroxycarmalol attenuated cell damage against UVB radiation via enhancing antioxidant effects and absorbing UVB ray in human HaCaT keratinocytes. Environ Toxicol Pharmacol 2013;36:680-688.

Piao MJ; Lee NH; Chae S; Hyun JW. Eckol inhibits ultraviolet B-induced cell damage in human keratinocytes via a decrease in oxidative stress. Biol Pharm Bull 2012;35:873-880.

Piao MJ; Susara Ruwan Kumara MH; Kim KC; Kang KA; Kang HK; Lee NH; Hyun JW. Diphlorethohydroxycarmalol suppresses ultraviolet B-Induced matrix metalloproteinases via inhibition of JNK and ERK signaling in human Keratinocytes. Biomol Ther 2015a;23:557-563.

제주대학교 중앙도서관
JEJU NATIONAL UNIVERSITY LIBRARY

Puri P; Nandar SK; Kathuria S; Ramesh V. Effects of air pollution on the skin: a review. Indian J Dermatol Venereol Leprol 2017;83:415-423.

Ryu YS; Kang KA; Piao MJ; Ahn MJ; Yi JM; Bossis G; Hyun YM; Park CO; Hyun JW. Particulate matter-induced senescence of skin keratinocytes involves oxidative stress-dependent epigenetic modifications. Exp Mol Med 2019a;51:108.

Ryu YS; Kang KA; Piao MJ; Ahn MJ; Yi JM; Hyun YM; Kim SH; Ko MK; Park CO; Hyun JW. Particulate matter induces inflammatory cytokine production via activation of NFκB by TLR5-NOX4-ROS signaling in human skin keratinocyte and mouse skin. Redox Biol 2019b;21:101080.

Sanjeewa KKA; Kim EA; Son KT; Jeon YJ. Bioactive properties and potential cosmeceutical applications of phlorotannins isolated from brown seaweeds: A review. J Photochem Photobiol B 2016;162:100-105.

Sano R; Reed JC. ER stress-induced cell death mechanisms. Biochim Biophys Acta 2013;1833:3460-3470.

Schraufnagel DE; Balmes JR; Cowl CT; De Matteis S; Jung SH; Mortimer K; Perez-Padilla R; Rice MB; Riojas-Rodriguez H; Sood A; *et al.* Air pollution and noncommunicable diseases: A review by the forum of international respiratory societies' environmental committee, part 2: Air pollution and organ systems. Chest 2019;155:417-426.

Shin EJ; Tran HQ; Nguyen PT; Jeong JH; Nah SY; Jang CG; Nabeshima T; Kim HC. Role of mitochondria in methamphetamine-induced dopaminergic neurotoxicity: Involvement in oxidative stress, Neuroinflammation, and pro-apoptosis-a review. Neurochem Res 2017;43:57-69.

Shrestha A; Pun NT; Park PH. ZFP36L1 and AUF1 induction contribute to the suppression of inflammatory mediators expression by globular adiponectin via autophagy induction in macrophages. Biomol Ther 2018;26:446-457.

제주대학교 중앙도서관
JEJU NATIONAL UNIVERSITY LIBRARY

Sun L; Fu J; Lin SH; Sun JL; Xia L; Lin CH; Liu L; Zhang C; Yang L; Xue P; *et al.* Particulate matter of 2.5 μm or less in diameter disturbs the balance of TH17/regulatory T cells by targeting glutamate oxaloacetate transaminase 1 and hypoxia-inducible factor 1α in an asthma model. J Allergy Clin Immunol 2020;145:402-414.

Sun Y; Liu WZ; Liu T; Feng X; Yang N; Zhou HF. Signaling pathway of MAPK/ERK in cell proliferation, differentiation, migration, senescence and apoptosis. J Recept Signal Transduct Res 2015;35:600-604.

Tang J; Yao C; Liu Y; Yuan J; Wu L; Hosoi K; Yu S; Huang C; Wei H; Chen G. Arsenic trioxide induces expression of BCL-2 expression via NF-κB and p38 MAPK signaling pathways in BEAS-2B cells during apoptosis. Ecotoxicol Environ Saf 2021;222:112531.

Trachana V; Petrakis S; Fotiadis Z; Siska EK; Balis V; Gonos ES; Kaloyianni M; Koliakos G. Human mesenchymal stem cells with enhanced telomerase activity acquire resistance against oxidative stress-induced genomic damage. Cytotherapy 2017;19:808-820.

Tsai MH; Hsu LF; Lee CW; Chiang YC; Lee MH; How JM; Wu CM; Huang CL; Lee IT. Resveratrol inhibits urban particulate matter-induced COX-2/PGE2 release in human fibroblast-like synoviocytes via the inhibition of activation of NADPH oxidase/ROS/NF-κB. Int J Biochem Cell Biol 2017;88:113-123.

Wang Y; Xiong L; Tang M. Toxicity of inhaled particulate matter on the central nervous system: neuroinflammation, neuropsychological effects and neurodegenerative disease. J Appl Toxicol 2017;37:644-667.

Wu Y; Song P; Lin S; Peng L; Li Y; Deng Y; Deng X; Lou W; Yang S; Zheng Y; *et al.* Global burden of respiratory diseases attributable to ambient particulate matter pollution: Findings from the Global Burden of Disease Study 2019. Front Public Health 2021;9:740800.

제주대학교 중앙도서관
JEJU NATIONAL UNIVERSITY LIBRARY

Xie X; Zu X; Liu F; Wang T; Wang X; Chen H; Liu K; Wang P; Liu F; Zheng Y; *et al.* Purpurogallin is a novel mitogen-activated protein kinase kinase 1/2 inhibitor that suppresses esophageal squamous cell carcinoma growth in vitro and in vivo. Mol Carcinog 2019;58:1248-1259.

Xin Y; Guo W; Yang C; Huang Q; Zhang P; Zhang L; Jiang G. Photodynamic effects of vitamin K3 on cervical carcinoma cells activating mitochondrial apoptosis pathways. Anticancer Agents Med Chem 2021;21:91-99.

Yang L; Zhang H; Zhang X; Xing W; Wang Y; Bai P; Zhang L; Hayakawa K; Toriba A; Tang N. Exposure to atmospheric particulate matter-bound polycyclic aromatic hydrocarbons and their health effects: A Review. Int J Environ Res Public Health 2021;18:2177.

Yao W; Lin Z; Wang G; Li S; Chen B; Sui Y; Huang J; Liu Q; Shi P; Lin X; *et al.* Delicaflavone induces apoptosis via mitochondrial pathway accompanying G2/M cycle arrest and inhibition of MAPK signaling cascades in cervical cancer HeLa cells. Phytomedicine 2019;62:152973.

Zhen AX; Hyun YJ; Piao MJ; Fernando PDSM; Kang KA; Ahn MJ; Yi JM; Kang HK; Koh YS; Lee NH; *et al.* Eckol inhibits particulate matter 2.5-induced skin keratinocyte damage via MAPK signaling pathway. Mar Drugs 2019a;17:444.

Zhen AX; Piao MJ; Hyun YJ; Kang KA; Fernando PDSM; Cho SJ; Ahn MJ; Hyun JW Diphlorethohydroxycarmalol attenuates fine particulate matter-induced subcellular skin dysfunction. Mar Drugs 2019b;17:95.

Zhen AX; Piao MJ; Hyun YJ; Kang KA; Ryu YS; Cho SJ; Kang HK; Koh YS; Ahn MJ; *et al.* Purpurogallin protects keratinocytes from damage and apoptosis induced by Ultraviolet B radiation and particulate matter 2.5. Biomol Ther 2019c;27:395-403.

Zheng JH; Viacava Follis A; Kriwacki RW; Moldoveanu T. Discoveries and controversies in BCL-2 protein-mediated apoptosis. FEBS J 2016;283:2690-2700.

제주대학교 중앙도서관
JEJU NATIONAL UNIVERSITY LIBRARY

ACKNOWLEDGMENTS

Since I came to Jeju National University for the first time in Feb 2017, it's been 6 years. I feel so lucky to have had a chance to study here for integrated Master's & Ph.D. courses, and finally, I got the degree of Ph.D. in Medicine.

There are too many people that I have to say thanks to. First of all, members of the Biochemistry Lab, Prof. Hyun Jin Won, Dr. Piao Mei Jing, Hyun Yu Jae, Sameera (Pincha Devage Sameera Madushan Fernando), and Lakmini (Herath Mudiyanselage Udari Lakmini Herath). I would like to express my deepest appreciation to Prof. Hyun Jin Won for supporting and teaching me here, and she is so professional at work and good support for students, from whom I learned a lot. Secondly, I want to thank Mei Jing teacher, who is a real helper to me and that teach and enlighten me in my tough life. And I thank Yu Jae eonni who taught me and help at the very first two years, and she is such a nice person whenever I think about her. Finally, I would say thank you to such an adorable couple, Sammera and Lakmini, who accompany me here and support me as well. I wish they would have a bright future and live a happy life. I would like to thank all professors, who taught me over the past 6 years as well.

I have met many grateful people after entering the university. I have to say that Prof. Li Yong is my first guide in inspiring my passion for a career in life science. I would express my deepest thanks for his generous help when I was a young girl. I would also thank my friends who accompanied me during the study period.

I would thank my family members, my parents, my parents-in-law, and my brothers, who give me the most selfless love and support. I would say thank you to my husband, who is such a special existence in this world to me and I couldn't love him more. I would say to myself that you are the best and you did it to learn not only knowledge but also life. I wish that I would continue to be brave, loving, and introspective in the future.

제주대학교 중앙도서관
JEJU NATIONAL UNIVERSITY LIBRARY

Finally, I would say thank you and sorry to my baby son, Pidan (Wu Yu Ze). After giving you birth, I could not take good care of you and left you for 1 and a half years without seeing each other at a such young age. I wish that I would stay with you and accompany you till you grow up. I love you and your father forever!

제주대학교 중앙도서관
JEJU NATIONAL UNIVERSITY LIBRARY

致 谢

回首在韩国济州国立大学就读硕博学位的这 6 年中，时光飞逝，感慨良多。此时，我的学校生活即将落幕，在此我将对所有帮助过我的人致以深深的感谢！

首先我将感谢玄鎭媛教授，是您的支持与帮助使得我的渡过了充实又愉快的 6 年学习生活。从您身上学到的专业知识以及向上的精神将使我终身受益。其次我要感谢朴美京博士，您是我最坚实的后盾，是我向前的动力，没有您的指导与陪伴，那这六年的生活将会变成一种遗憾。我也将感谢送给其他实验室成员，包括我的师姐현유재，以及这对可爱的夫妇 Sammera 和 Lakmini。感谢你们的陪伴以及共同渡过的美好时光。我也将感谢所有在我硕博期间授课的教授们。

在这里获得医学博士学位的契机，让我不得不提我的硕士研究生导师李勇教授，是您点燃了我对生命科学领域的激情。我要感谢您对年少的我慷慨的帮助以及支持。我还要感谢所有在我学习之路上给予过我支持和陪伴的朋友们，美好的回忆让我对过去充满了感激之情。

我也要感谢我的家人，我的父母以及我的兄长，是你们给予了我最无私的支持与爱。我也要感谢我人生中最重要的两个人，我的丈夫和我的儿子，感谢你们的理解和支持！最后我想对自己说一声，谢谢，感谢你的成长，感谢你的努力！

学校生活的结束，并不代表学习的结束，未来是新生活、新挑战的开始。路漫漫其修远兮，吾将上下而求索！

제주대학교 중앙도서관
JEJU NATIONAL UNIVERSITY LIBRARY